

# POLITECNICO DI TORINO

Corso di Laurea Magistrale  
in Ingegneria biomedica

Tesi di Laurea Magistrale

Characterization and optimization of a miniaturized  
microscope-integrated bioreactor for the generation of  
functional engineered cardiac tissues



**Relatori** Prof. Umberto Morbiducci

**Correlatori** Dr. Anna Marsano

Dr. Diana Massai

Dr. Giuseppe Isu

**Candidato**

Alessia Pisanu

Luglio 2018

*A mia madre e a mio padre*

*A mia sorella Fabiana*

# CONTENTS

---

<b>1</b>	<b>Introduction</b>	<b>4</b>
1.1	State of art	4
1.1.1	Cardiac tissue engineering	4
1.1.2	Bioreactors and devices for CTE	8
1.2	Aim of the thesis	10
<b>2</b>	<b>Characterization and optimization of a miniaturised microscope-integrated bioreactor for mechanical training of engineered cardiac tissues</b>	<b>12</b>
2.1	Bioreactor description	12
2.1.1	Bioreactor's main features	12
2.1.2	Material composition	24
2.1.3	Image-based monitoring unit	26
2.1.4	Microscope as a displacement sensor	29
2.2	Bioreactor functioning mechanism	33
2.2.1	Auxotonic stimulation module	33
2.2.2	Isotonic stimulation module	37
2.2.3	Electrical stimulation module	55
<b>3</b>	<b>Effects of combination of auxotonic and isotonic mechanical stimulation on maturation and contractile properties of engineered cardiac tissue – a proof of concept</b>	<b>60</b>
3.1	Introduction	60
3.2	Material and Methods	62
3.2.1	Device sterilization	67
3.2.2	Neonatal rat cardiomyocytes isolation	67
3.2.3	Fibrin-based cardiac tissues generation	68
3.2.4	Biomechanical stimulation of the ECT	71
3.2.5	ECT characterization	74
3.3	Results	83
3.3.1	Histological results	83
3.3.2	Electrical pacing result	84
3.3.3	Force measurement results	86
3.4	Discussion and conclusions	87

4	Conclusions and future prospective	91
4.1	Miniaturized microscope-based bioreactor for mechanical training of engineered cardiac tissue	91
4.2	Proof of concept	92
4.3	Limitations	93
4.4	Future works	95
5	Acknowledgements	97
6	Appendix	99
7	Bibliography	104

# 1 INTRODUCTION

---

## 1.1 STATE OF ART

Cardiovascular diseases (CVD) represent 30% of the worldwide death and 10% of the cause of disability, with an increasing trend. Within CVD diseases, pathologies in the coronary artery are the most common, and myocardial infarction (MI) is the main leading cause of mortality in the Western World (*Roger, et al. 2012. Massai, et al. 2013*). MI presents a progressive cardiac function deterioration leading to an irreversible death of a portion of the heart tissue. After myocardial infarction, the cardiac tissue has limited capacity to regenerate itself, since it is poor in muscle stem cells, and cardiomyocytes are terminally differentiated cells with no proliferative capacity.

The current approaches to restore the heart tissue functionality are based on reperfusion treatments and on pharmacological therapies. However, traditional strategies, such as the implantation of left ventricular assist devices (LVAD) or heart transplantation, have limited durability and are often not feasible. This scenario motivates the research on the development of innovative treatments for cardiac injury.

In the last years, cardiac tissue engineering (CTE) has played an important role in this research field because it aims to create an in vitro cardiac tissue model useful for drug discovery and drug screening in the context of cardiac diseases.

### 1.1.1 Cardiac tissue engineering

The term “Tissue engineering” was introduced by the US National Science Foundation (NSF) and it was defined as “Application of principles and methods of engineering and life sciences toward fundamental

understanding of structure–function relationship in normal and pathological mammalian tissues and the development of biological substitutes to restore, maintain, or improve functions” (*Eschenhagen and Zimmermann, 2005*).

The CTE main aim is the generation of a 3D tissue that mimics the native heart tissue with similar properties and functionalities. It has been demonstrated that to obtain a functional cardiac engineered tissue, it is essential to implement a biomimetic approach simulating the physical stimulations present in the heart. Therefore, mechanical and electrical stimulations appear fundamental in the generation of heart tissues.

It has been shown that mechanical stimulation appears a potent regulator in the cardiac morphogenesis (*Zimmermann, et al 2013*). It leads to a favourable effect of cell differentiation and orientation when repetitive cycles of stretch and relaxation are imposed (*Vandenburgh, et al. 1988. Terracio, et al. 1988. Eschenhagen, et al. 2005*). Moreover, mechanical stimuli improve tissue maturation, enhance expression of junctional proteins and increase the active systolic force (*Stoppel, et al. 2015. Zimmermann, et al. 2013*). The native myocardium is indeed continuously exposed to hemodynamic load, especially during the early heart development phase. Equally, in cardiac engineered tissue, the biological response due to the mechanical load seems to depend on the developmental stage of the cardiomyocytes (*Zimmermann, et al. 2013*).

Physiological load could occur in different conditions. In the last decade, the Eschenhagen group carried out an important research study in the context of cardiac tissue engineering imposing cyclical mechanical loads to neonatal rat cardiomyocytes (NRCM) embedded in ring-shaped tissue constructs. Moreover, the myocardial tissues have been developed also in combination with NRCM (*Shimko, et al. 2008. Zimmerman, et al. 2002. Salameh, et al. 2010*), mouse and human embryonic stem cell-derived cardiomyocytes (*Shimko, et al. 2008*) to increase engineered cardiac tissue contractile performance.

Up to now, in literature mechanical stimulation protocols have been tested to encourage and to improve the maturation, the morphology and the functionality of the cardiac engineered tissues:

- a) auxotonic stimulation condition was implemented using flexible poles between the embedded cardiomyocytes; the bending poles make possible the generation of the cardiomyocytes passive force, because they start to develop a force as much as they are mature;
- b) isotonic stimulation condition implemented using phasic moving poles that are connected to the tissue and on which a cyclical stretch is imposed to mimic the native tissue condition.

Therefore, auxotonic stimulation represents an indirect stimulation condition, because it is not controlled externally but it is fundamental to guarantee the tissue maturation and the cells contractile force development. Regarding the second mechanical stimulation condition, it imposed an active, cyclic and controlled strain on the cardiac tissue. The latter can adapt to the load cycle and this condition represents a training for it.

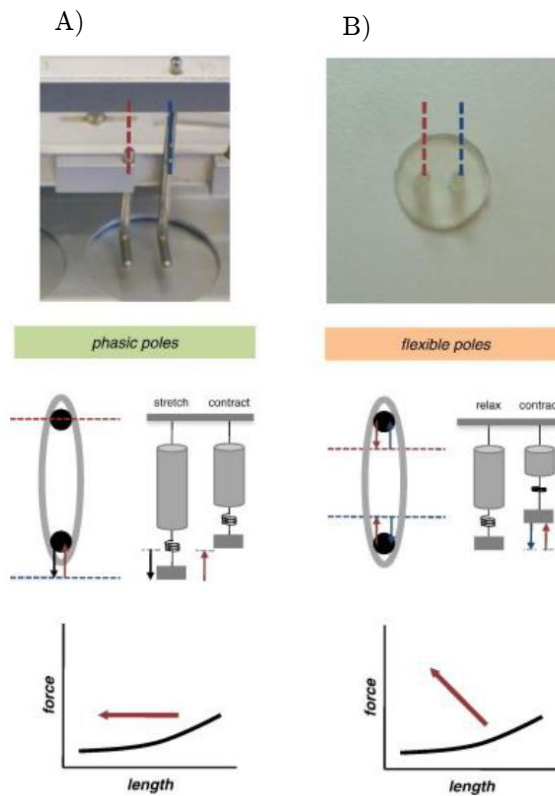


Figure 1.1: Different loading protocols tested in literature. A) Isotonic stimulation under a phase reset of the cardiac tissue length; B) auxotonic constriction enabled by suspension of the cardiac tissue on flexible poles. (N. Y. Liaw and W.H. Zimmermann, 2015).

To apply the described loading protocols, there is the need to exploit suitable instrumentation. In this context, bioreactors have become indispensable tools to apply successful strategies, enabling the monitoring and the control of the tissue physico-chemical environment and providing a wide range of physical stimuli (Massai, et al. 2013).

### 1.1.2 Bioreactors and devices for CTE

The introduction of specific instruments was necessary to produce three-dimensional engineered cardiac tissues (ECT) and to standardize the processes behind their generation. Among these instruments, one of the most important in the context of the Regenerative Medicine (RM) is the bioreactor. Segen's Medical Dictionary defines the latter as "a closed reaction vessel for fermentation or enzymatic reactions for production of cells and biosynthetic products" and as instruments that "allow automatic regulation of the flow of oxygen, culture medium and other nutrients, and maintaining the temperature and pH". Moreover, bioreactors minimize potential contaminations and they are able to generate a higher density of cells than typically produced in traditional cultures (*Segen's Medical Dictionary, 2012 Farlex, Inc.*).

As mentioned before, bioreactors play an essential role in CTE, since generation of cardiac tissue is characterized by complex structure and function, it is not feasible by using only Petri dish systems for cell culture. In fact, without the suitable physical stimuli cells could not organize themselves within the 3D tissues (*Bilodeau, et al. 2006*). Bioreactors allow to monitor the environment and the properties of the cardiac engineered tissue construct, but they also can physically stimulate it in order to provide the features that mark the natural cardiac tissue.

A proper bioreactor design to generate in vitro cardiac tissue models and to analyse the biological environment and the effects of the stimulation must be closely defined, standardized and as much as possible operator-independent. It should guarantee:

- a) reproducibility,
- b) scalability,
- c) safety in terms of contamination risk,
- d) automaticity and repeatability of the processes.

So far, several bioreactors have been developed to generate 3D ECT and for the application of controlled mechanical stimulation on them. Most of these devices were characterized by bulky architecture and large size that allow a wide range of stimulation together with a depth macroscale analysis (*Bose and Ebers bioreactors*). On the other hand, the bulky architecture and the lack of flexibility on their implementation:

- a) make difficult to obtain real-time monitoring using the traditional microscopy systems,
- b) avoid a microscale investigation of the construct,
- c) lead to a limited stimulation patterns.

Furthermore, in literature were implemented other kind of instruments to develop a 3D heart model. They are micro-fluidic devices able to create micro three-dimensional models to mimic the fibrotic cardiac tissue. The microscale of these device drives to the main advantages to work with a higher control over the tissue environment and with an effective reduction in the use of the compounds (*Marsano, et al. 2016*). Although the mentioned microdevices guarantee a depth molecular readout, they suffer from the limited range of stimulation, difficult usability, and poor functional readout.

On the view of the already existing tools, nowadays the aim is to obtain an in vitro biomimetic tissue generation strategy able to provide both microscale and macroscale evaluations.

## 1.2 AIM OF THE THESIS

The aim of the thesis is to characterize the functionalities of a miniaturized bioreactor for applying different physical stimulation conditions to mesoscale 3D cardiac engineered tissues, promoting their environment and maturation.

To implement it, the bioreactor design was conceived to be integrated in traditional microscopy systems: the modular architecture can be fitted in traditional plastic culture dishes and used directly under the microscope to monitor the construct. The device modularity and integrability drove an important decrease of the using costs and of the implementation costs because it reduced the need to have additional sensors that normally should support the bioreactor functioning. More precisely, the dynamic stimulation but also the contractile force of the construct can be respectively monitored and evaluated with a displacement sensor implemented using a live-imaging microscope. Furthermore, to obtain an average measure of the developed force of the heart tissue, it was necessary to equip the device with a force measurement sensor. Still, the microscope analysis was exploited to evaluate a cantilever sensor displacement.

Therefore, the bioreactor design aimed at obtaining a device in which it is possible to provide mechanical and electrical stimulation on the engineered ex vivo heart tissue and to measure the effects of the physical stimulation in terms of biological response and tissue functionality.

The 3D myocardial engineered tissue was realized as a hydrogel-based cardiac tissue. It was generated using a fibrin gel in which the cardiomyocytes are embedded. Several in vitro studies have indeed demonstrated that fibrin gel-based construct promoted cell migration, proliferation and matrix synthesis (*Mandel, et al. 1997*). Moreover, the mentioned hydrogel-based construct drives to many advantages for tissue engineering application and is indeed widely used for different tissue model generation (*Ahmed, et al. 2008*). Concerning ECT, the cardiomyocytes

surrounded into fibrin construct have shown a strong capability of compacting, remodelling and creating extracellular matrix (*Ye, et al. 2000*).

The miniaturized integrated-based bioreactor project has been developed and then implemented by the Cardiac Surgery and Engineering research group at the Department of Biomedicine of University of Basel (Switzerland), while the thesis project was focused on the physical and mechanical characterization of the bioreactor and of its main functioning modules, on the optimization of the device and of the components design:

- a) optimization and realization of the main prototyping elements of the device,
- b) optimization and characterization of the actuator used in the dynamic stimulation system,
- c) standardization and calibration of an acquisition system as displacement sensor,
- d) calibration of the force measurement sensor,
- e) evaluation of the construct biological response,
- f) analysis and characterization of the biological response.

Afterwards, the final aim of the thesis has been the biological validation of the bioreactor as a first proof of concept.

## 2 CHARACTERIZATION AND OPTIMIZATION OF A MINIATURISED MICROSCOPE-INTEGRATED BIOREACTOR FOR MECHANICAL TRAINING OF ENGINEERED CARDIAC TISSUES

---

### 2.1 BIOREACTOR DESCRIPTION

#### 2.1.1 Bioreactor's main features

In this chapter, the microscope-integrated bioreactor is described. The bioreactor was designed for mechanical stimulation of three-dimensional ECT and in order to be integrated in microscopy systems and standardized laboratory plasticware materials used in the cell culture context (i.e. culture dishes and plates). The main requirements that have driven the design were:

- a) to guarantee the cells surviving and then to facilitate their capability to create a new functional tissue,
- b) to maintain standard culture conditions,
- c) to mechanically and electrically stimulate the construct,
- d) to measure and to characterize the construct biological response.
- e) to measure and monitor functional parameters (e.g. contractile and passive force) within the bioreactor with non-destructive methods.

#### **Bioreactor frame**

One of the main requirements on which the design is based is the bioreactor frame's shape and size. As previously stated, it was designed in order to be able to be integrated in standard cell culture dishes. This requirement drives to important advantages in the TE context, because it guarantees:

- a) to easily analyse what happens during the bioreactor use because of the possibility of using standard tools,
- b) to perform the cell culture experiments directly inside the traditionally used dishes,
- c) to upscale the experiment system and the device to different dishes size.

Regarding the last two concepts (b, c), the prototype of the bioreactor was designed to have modular features: it was designed as a modular component with a size suitable for the round-shape Petri dishes with 56 cm<sup>2</sup> culture area. This frame is characterized by rectangular chambers (37 mm x 53 mm x 15 mm) and they are isolated from the bottom of the culture dish by a polymeric membrane that is based in the bottom of the bioreactor avoiding contaminations due to culture medium stagnation. The chamber hosts the culture medium and the construct is suspended on it, accommodated between two metal posts held by two different mounting pieces. Both the metal posts and the mounting pieces properties will be described in the following sub-chapter.

*Figure 2.1* shows the design of the bioreactor frame and its main components.

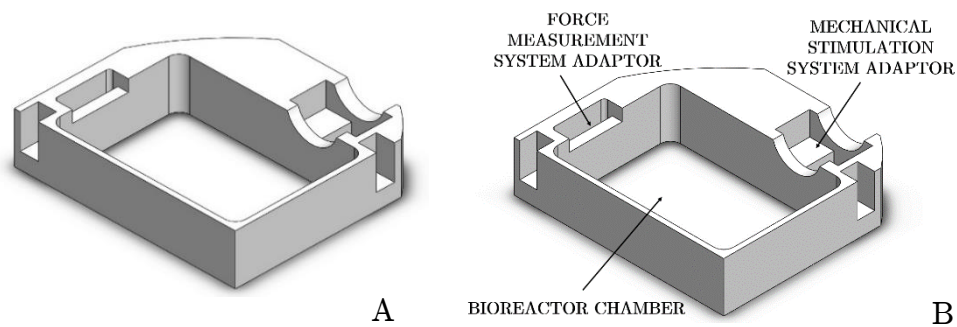
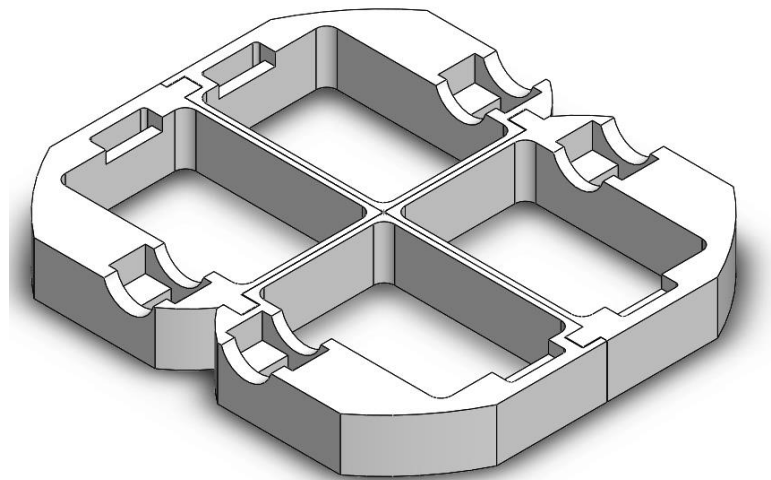


*Figure 2.1* Isometric view of the Solidworks mono-chamber bioreactor model (A) and scheme of the main frame's parts (B).

As highlighted in Figure 2.1, , the frame design allows to implement a mechanical stimulation module and force transducer module in order to fulfil requirements c), d)and e) of paragraph 2.1.1.

The described modular bioreactor frames can be mounted together in order to constitute a four wells-bioreactor (*Figure 2.2*). In this way, the user can exploit the bioreactor frame to implement one-well experiment and combine the single well-frame to obtain four independent 3D replicates.



---

*Figure 2.2 Isometric view of the Solidworks 4 well-bioreactor model assembly.*

This design was the first design of the frame proposed for the generation of a functional prototype. The frame represents only a support for the mechanical stimulation and the force transducer modules, and it does not interfere with the functionality of the two modules. Indeed, this modular approach allowed to validate the functionality of the system, keeping open future implementations or redesign of the frame (see paragraph 3.2).

## Bioreactor functioning modules

As mentioned before, the ECT was conceived as a hydrogel-based tissue (*Figure 2.3*). The cardiomyocytes were suspended inside a fibrin gel that was included with compounds necessary for the polymeric matrix generation. The stated components and their functionality for the phases of the gel formation will be described in the dedicated chapter about the biological validation of the bioreactor.

The fibrin-based cardiac tissue was positioned inside the bioreactor culture chamber, casted around two metal posts (*Figure 2.4*).

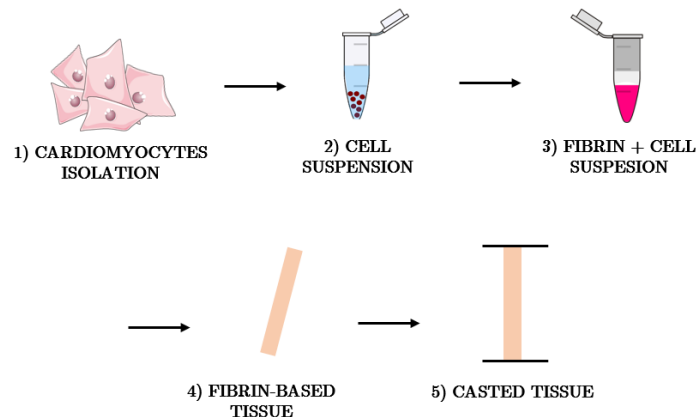


*Figure 2.3 Fibrin-based cardiac tissue generation main steps and casting around the metal posts.*

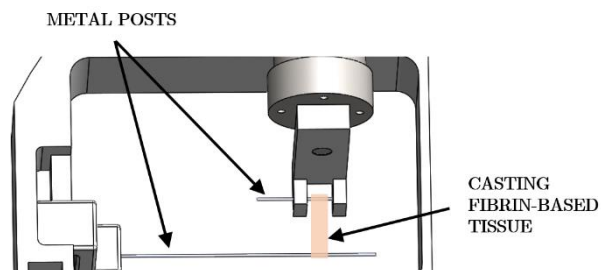


*Figure 2.4 Scheme of the fibrin-based cardiac tissue casted around the metal posts.*

The posts are Nichel-Titanium alloy wires (Nitinol). This is a shape memory alloy (SMA) and it is a biomaterial very commonly employed in several biomedical fields. The Nitinol posts have been implemented as 0.4 millimeters diameter wires. They allow the linear and stable positioning of the construct, preventing its migration. At the same time, their efficient mechanical and electrical properties have made possible the implementation of the three modules that characterize the bioreactor functioning.

The posts are indeed two wires of different length (a long one and a shorter one):

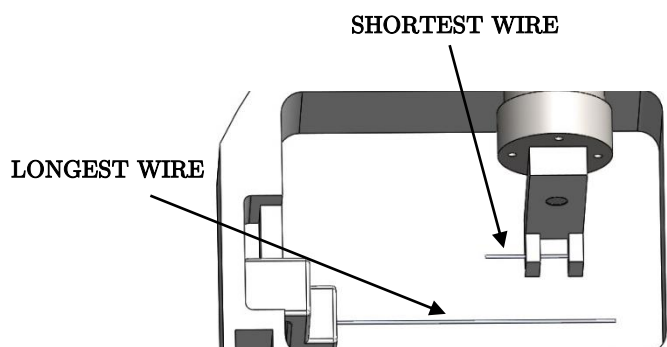


*Figure 2.5 Scheme of the bioreactor frame model and the Nitinol wires positioning.*

The longest wire was exploited to implement the auxotonic mechanical stimulation of the ECT (*Figure 2.6 (A)*). More precisely, it was exploited the flexibility property of the Nitinol: when the cells start to develop a passive force  $F$  and they start to pull, the wire can deflect, as shown in the following scheme (*Figure 2.6 (A)*). In this way, the wire deformability promotes the self-remodeling of the cardiomyocytes into the hydrogel tissue.

On the other side, the second wire (shorter and fixed to a clamp component) played an essential role on the implementation of the second

module of mechanical stimulation implementing a mechanical isotonic stimulation by cyclical tissue stretching. As the following figure highlights (*Figure 2.6 (B)*), to implement that, the shortest Nitinol wire is clamped to an actuator. The latter can produce a strain on the tissue imposing a back and forth displacement (with a precise stretch percentage and frequency value). That principle of functioning permits to apply cyclic loading to the tissue, simulating the physical stimuli that are present in the heart.

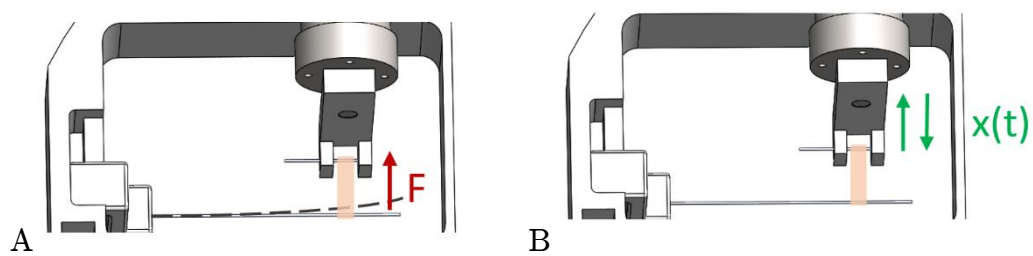


*Figure 2.6 Scheme of the auxotonic stimulation condition (A) and of the isotonic (B) implementation on the ECT embedded between the Nitinol wires. In the auxotonic condition, the passive force of the construct produces the bending of the longest poles, while in isotonic condition, the displacement  $x(t)$  back and forth imposes a cyclic stretch of the tissue.*

Although the mechanical stimulation and the force transducer module function independently from one another, from their union derives a third module. Indeed, the performing electrical properties of the Nitinol support their use as electrodes. Since the heart tissue presents both mechanical and electrical properties, the imposition of an electrical pacing directly through the use of the Nitinol wires allows for the evaluation of the tissue contractile force within the bioreactor chamber, without the need of new components.

### **Bioreactor module main components**

As already stated before, the main component that ensures the auxotonic stimulation, thus the passive force and structure organization of the

developing tissue is a long Nitinol wire. The latter was inserted in the frame by a suitable holder that was designed to:

- a) be easily mounted into the bioreactor frame,
- b) bind to the Nitinol wire.

Therefore, the wire holder described in the *Figure 2.7* can be positioned by the user directly entering from above thanks to the adapters present in the frame, as summarized by the schemes in figure (*Figure 2.8*). In fact, the frame presents a pocket fitting the shape of these components' fin part.

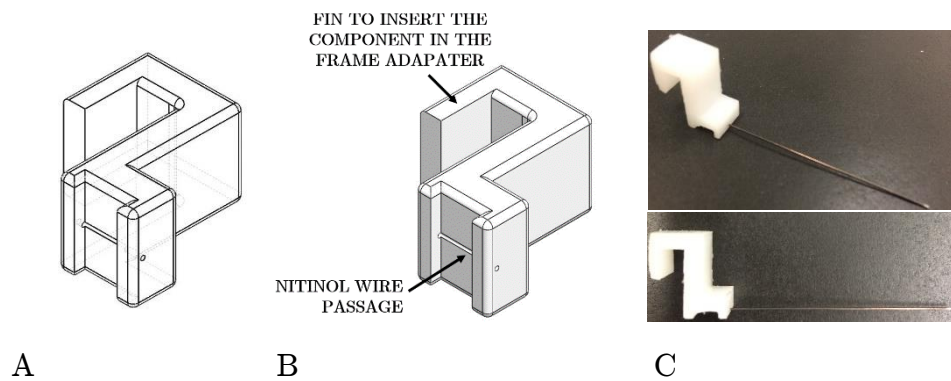


*Figure 2.8 Wire holder component: Solidworks drawing (A) and descriptive scheme of the model (B); pictures of the piece: holder (in white) and wire(C).*

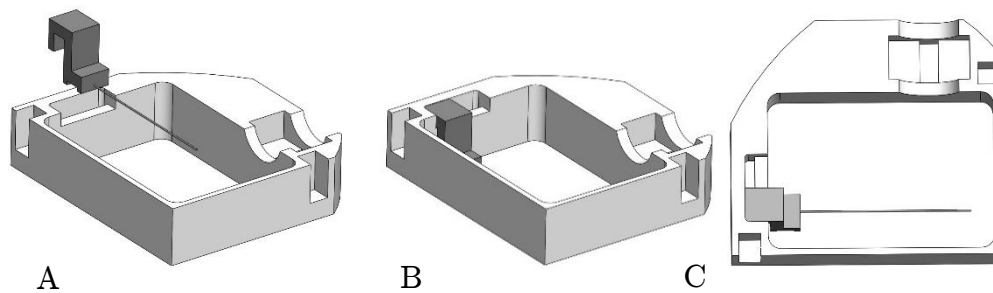
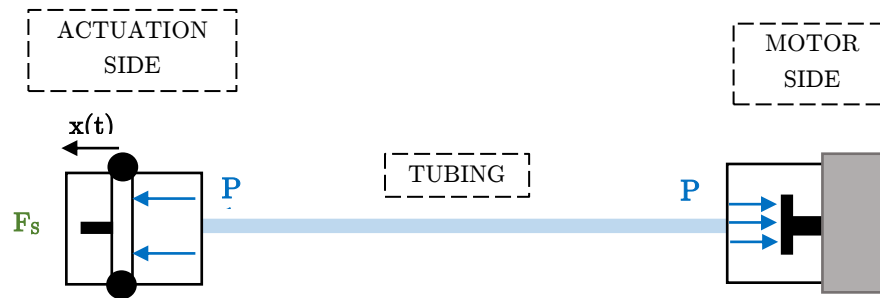


*Figure 2.7 Wire holder component on the frame adaptor: Solidworks model of the frame and the wire holder (A); Solidworks assembly of the components in isometric view (B) and from above (C).*

To implement the cyclic stretching movement a hydraulic syringe-like piston was designed and characterised (see *Scheme 2.1*). It was implemented by:

- a) a motor that drives the desired motion which is not in contact with the culture environment,
- b) an actuator which delivers the desired motion inside the culture environment,
- c) a non-compliant tubing in order to link the previous mentioned parts which can be easily put far away from each other



*Scheme 2.1 Hydraulic actuation system scheme: engine, tubing and actuation side; pressure of the fluid ( $P$ ) and imposed force of the spring ( $F_s$ ).*

The use of an hydraulic actuator was conceived to allow for the generation of cyclic actuation by simply using syringes and syringe-pumps to generate a pulsed motion.

Indeed, at the beginning, as a proof of concept, the actuation was implemented using a commercial syringe pump device (*Harvard Apparatus* produced) able to drive a syringe (i.e. the driving part). Connecting the syringe through the rigid tubing to a piston actuator, the motion is easily delivered to the culture environment.

The choice to use a hydraulic syringe-like piston device as mechanical stimulation system permits to avoid the rigid transmission chains between

motor side (in remote position) and the loading constructs inside the bioreactor chamber. The absence of rigid kinematics is meant to favour the implementation of the functioning system under any kind of microscope in an efficient mode. Moreover, the hydraulic system works as a damper for natural vibration bringing the desired motion without significant vibrations, feature that is essential when observing the culture tissue at high magnification. Being the syringe pumps a widely used tool in the context of the tissue engineering, their ease of use makes the system suitable for any lab user also when it is necessary to set different functioning parameters and to drive several syringes.

The actuation side was implemented using a cylinder connected with the tubing (*Figure 2.9*). It was designed with a hollow part that can be filled by the hydraulic fluid and that hosted the piston element. Indeed, the latest could move along the inside part of the cylinder driven by the fluid flow generated by the hydraulic system. As the following figure highlights, the actuator cylinder was designed to be mounted on the bioreactor frame and to be easily removed, as well as for the wire holder element described before.

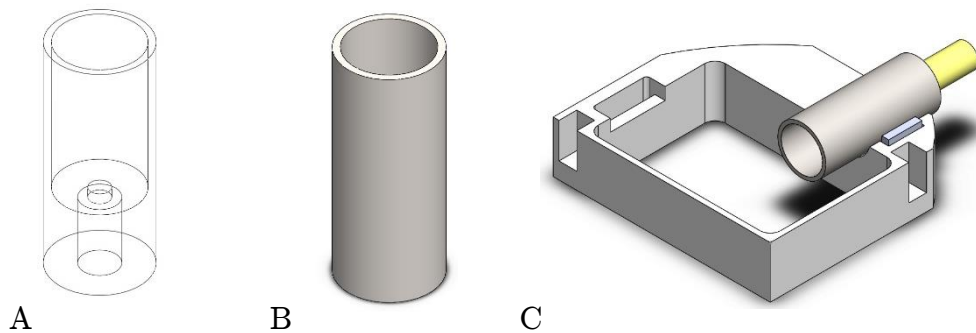


*Figure 2.9 Cylinder component model: Solidworks drawing (A) and model (B) of the component; assembly of the cylinder inserted into the frame of the bioreactor (C).*

The cylinders design and manufacturing were realized together with the other components that constitute the actuator part of the hydraulic system. In fact, as mentioned before, the cylinders were designed to accommodate the hydraulic fluid and the piston that is moved by the fluid's

displacement. The piston shown in the *Figure 2.10* was produced with the same material of the cylinder and it was designed with a short cylindrical part (with the same inner diameter of the cylinder) that includes a location for an o-ring element. The latter makes easier the piston's sliding back and forth, decreasing friction effects. The part that emerges from the inside of the actuator is like a long screw which is screwed on the actual piece to stimulate. Indeed, the cyclic displacement of the piston element driven by the fluid produced the translation of the tissue.

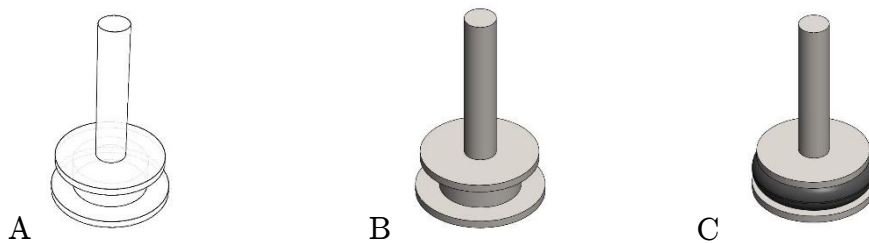


*Figure 2.10 Piston actuator component: Solidworks drawing (A) and model (B); Solidworks modelling of o-ring element insertion into the piston.*

At the beginning, the described cylinder components were designed with a different shape. In fact, they were characterized by the same hollow part for the piston, but with an elbow geometry that allow the connector screwing. This version (*Figure 2.11*) has been advantageous to the increased solidarity of the piece, but the presence of the angular shape has made less easy to implement the hydraulic fluid filling procedure in terms of dynamic of the fluid. The latter concept will be clearer in the description of the hydraulic system filling procedure.

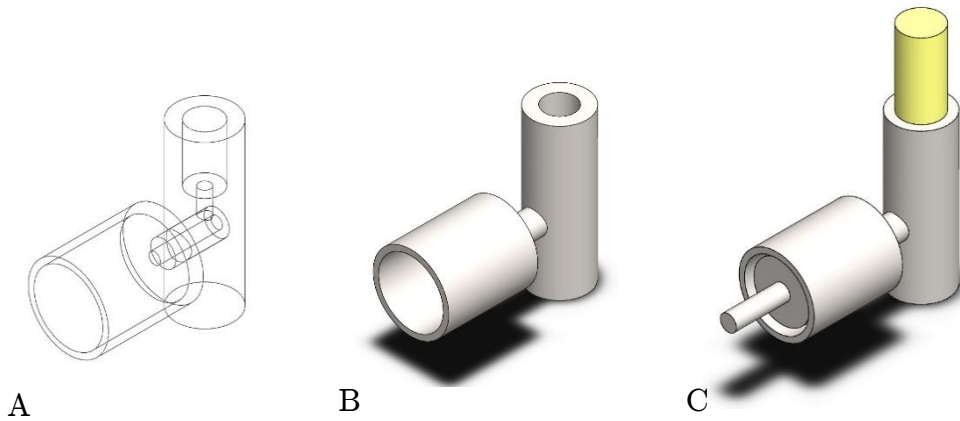


*Figure 2.11 Cylinder component model: Solidworks drawing (A) and model (B) of the component; assembly of the cylinder with the piston and the connector elements (C).*

The design of the bioreactor was planned to allow the use of both the cylinder versions.

The final part that completes the cylindrical component of the actuator is a cap that was designed in order to close the whole component and to make it a solid one (*Figure 2.12*). The cap fits in the final part of the cylinder and it presents a hole that allows the piston screw to stay outside and at the same time to maintain the correct position.

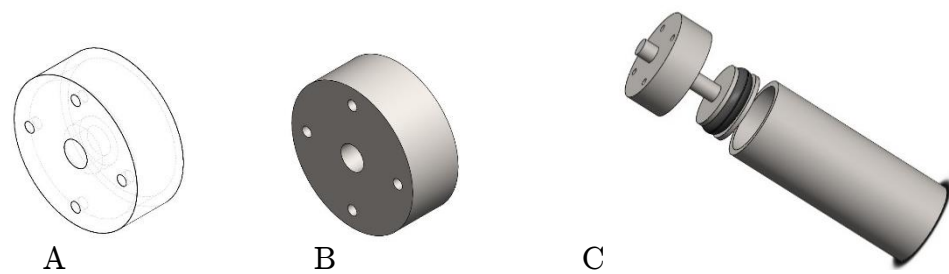


*Figure 2.12 Cylinder cap model: Solidworks drawing (A) and model (B); explosion view of the Solidworks assembly of the actuator component (C).*

Regarding the clamp, linked to the piston element, it is the piece in which the construct is held on (*Figure 2.13*). For this reason, it was designed to be screwed in the piston and to clamp the Nitinol rods that accommodate the ECT construct. The wires were fixed thanks to the clamps with a defined distance from the bottom of the culture dish that includes the bioreactor. The component is set in movement by the hydraulic actuator, thus allowing to stretch the tissue during the mechanical stimulation or holding it in position during static or quasi-static conditions. The Nitinol wires fixed to the clamps extending across a lateral side because they also have an important role in the external electrical stimulation of the construct.

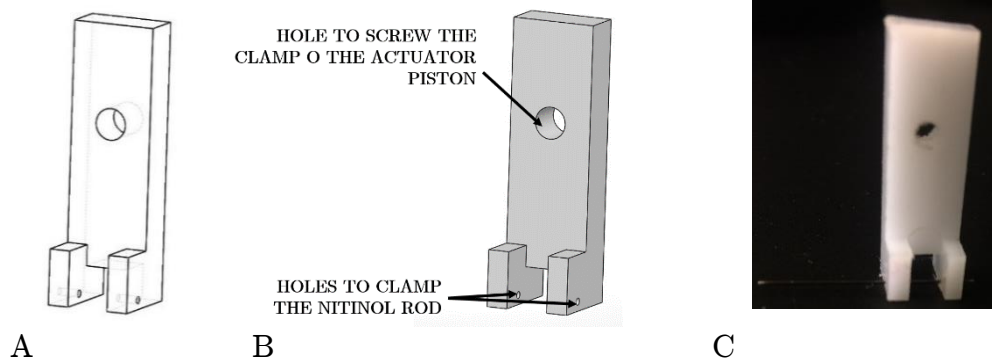


*Figure 2.13 Clamp component: Solidworks drawing (A) and descriptive scheme of the clamp (B); picture of the piece (C).*

The other end of the construct was clamped thanks to the rod that constitutes the cantilever, which is the force measurement module. It will be described in the next section (2.2.3). Indeed, in the following figure, it was reported a schematic view of the bioreactor frame with its modules and underlining the space on which the ECT could be positioned (*Figure 2.14*).

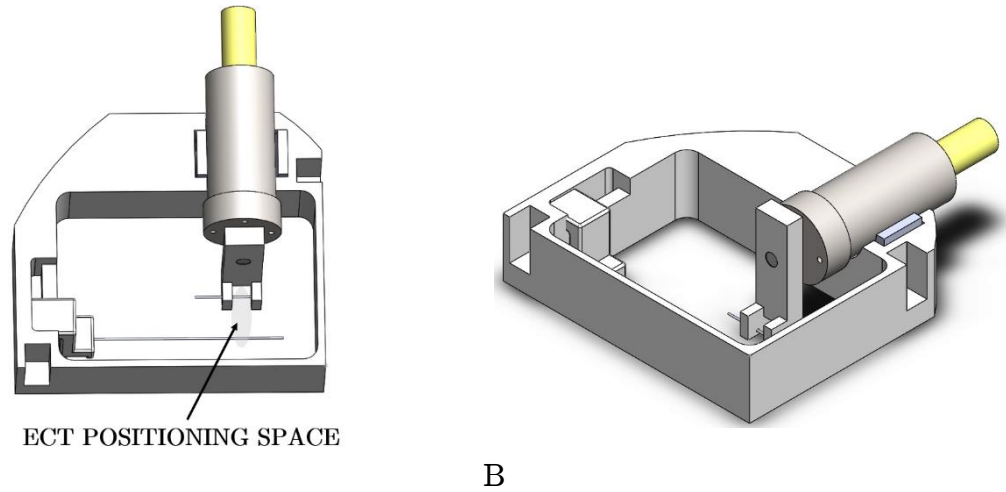


*Figure 2.14 Mono-chamber frame model: Solidworks model scheme (A) and isometric view of the Solidworks assembly (B).*

### 2.1.2 Material composition

The bioreactor was designed to be realized with safe materials, in terms of cytocompatibility, but also keeping in mind the requirements of:

- a) ease of sterilization of the components,
- b) ease of manufacture, to use and to monitor,
- c) scalability,
- d) prevention of culture medium leakage,
- e) cost effective and low cost of implementation.

The main material used for the bioreactor tools has been Polyoxymethylene (POM), also known as polyformaldehyde. It is a polyacetal polymer with a high flexural and tensile strength, stiffness, hardness, and excellent chemical resistance. Therefore, it is characterized by a low coefficient of friction, and good heat and fatigue resistance. Thanks to

its property, it is an easily sterilisable material, but also simply to manufacture.

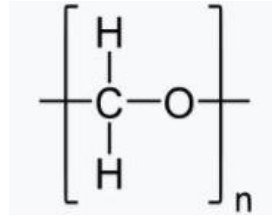


*Figure 2.15 Polyoxymethylene chemical formula.*

This polymer was used to realize the clamp components and the cantilever holder. These pieces were made thanks the Computer Numerical Control machine use (CNC) and the lathe and the drill press. The latter manufacturing machines were used to realize the other components of the device as the actuator components (cylinder, piston and cap) that were made in stainless steel. The latter has important features:

- a) biocompatible,
- b) sterilisable,
- c) excellent corrosion resistance,
- d) easy to lubricate,

and especially the properties c) and d) are fundamental in the context of the hydraulic systems use.

As a proof of concept, the bioreactor frames were 3D printed. More precisely, the prototype was modelled using the MakerBot Replicator+ printer with a Polylactide acid (PLA) 3D printing filament.

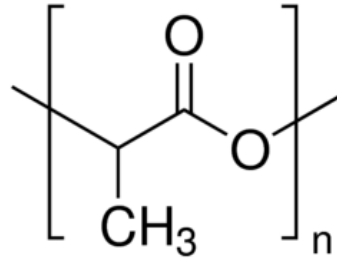


*Figure 2.16 PLA chemical formula*

The 3D printed frame was used to train the bioreactor in order to optimize the device functioning before to manufacture the definitive pieces.

Furthermore, since the bioreactor is positioned into a traditional Petri, between the two tools is necessary the presence of a material for the isolation of the wells to avoid fluid stagnation and communication among the different parts. The isolation was implemented thanks to the realized membrane of polydimethylsiloxane (PDMS): biostable polymer widely used in biomedical application.

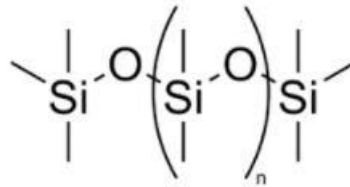


*Figure 2.17 Polydimethylsiloxane chemical formula.*

### 2.1.3 Image-based monitoring unit

To study and to monitor the operating mechanism of the bioreactor, it was necessary to analyse the constructs and their mechanical loading, carried out by the engine, through a displacement sensor. Given the miniaturized dimension of the system and the difficulties to integrate

miniaturized displacement sensors, a CCD microscope camera was used as displacement sensor to evaluate the stimulation actuator functioning by tracking its motion. To validate the image-based displacement sensor, a commercial microscope-camera was embedded in an already existing stereo-microscope structure (*Figure 2.18*): a 3D printed adaptor was designed to stabilize the camera in the microscope-frame structure, allowing a standardized and repeated measurements.



*Figure 2.18* Scheme of the acquisition camera placement into the microscope framework.

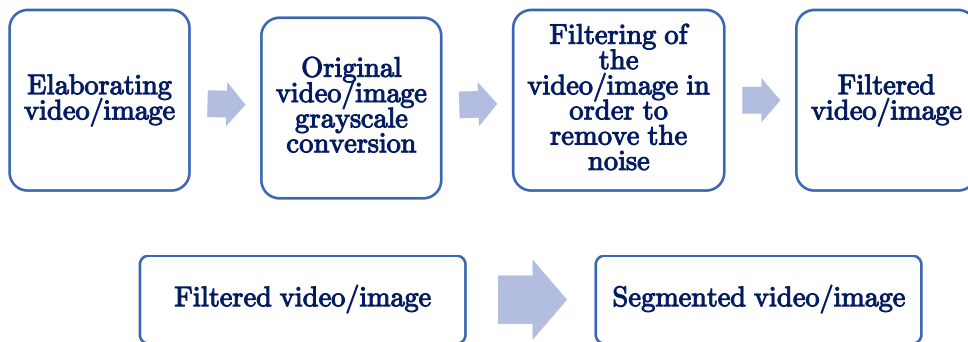
Moreover, the monitor unit was equipped with a high precision stage in which the bioreactor was positioned. Below the camera objective, the stage could move accurately the bioreactor in x-y direction into the microscope framework. In this way, the stage can be moved in exact and precise positions, to easily investigate the motion in each culture well of the bioreactor.

The acquisition system was preliminarily optimised with respect to:

- a) light intensity,

- b) contrast,
- c) camera position,
- d) camera framerate,

in order to distinguish a feature of the moving part of bioreactor and easily follow its movements. A recorded video is thus properly elaborated by an image-processing Matlab code written on purpose. As summarized in the following scheme (Scheme 2.2), each frame was elaborated and filtered in order to remove the background noise. Beginning from the system record (*Figure 2.19 (A, B)*), the camera was focused on the white element on which the fixed wire was clamped (*Figure 2.19 (C)*). Afterwards, the Matlab code has converted each frame of the video in greyscale and it has applied a filter on them. Then, it was possible to obtain a segmented image (*Figure 2.19 (D)*), using a routine based on the gradient of the frames.



*Scheme 2.2 Filtering and segmentation routine steps.*

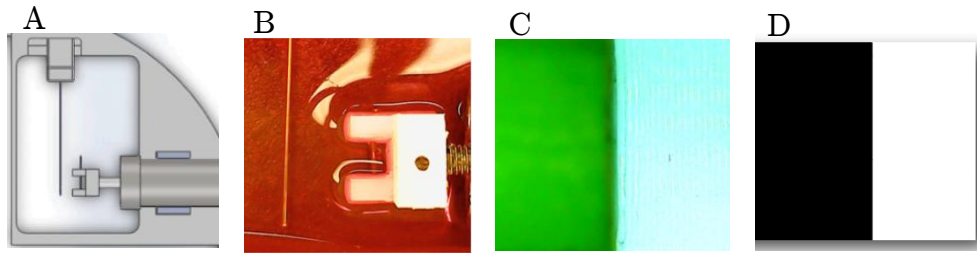


*Figure 2.19 Solidwork rendering from above of the bioreactor frame equipped with the instrumentation for the mechanical stimulation (A); recorded photoshoot from above of the same system with the detail of the actuator piston clamp (B); microscope view of the white clamp (C) and same view segmented using the image processing routine (D).*

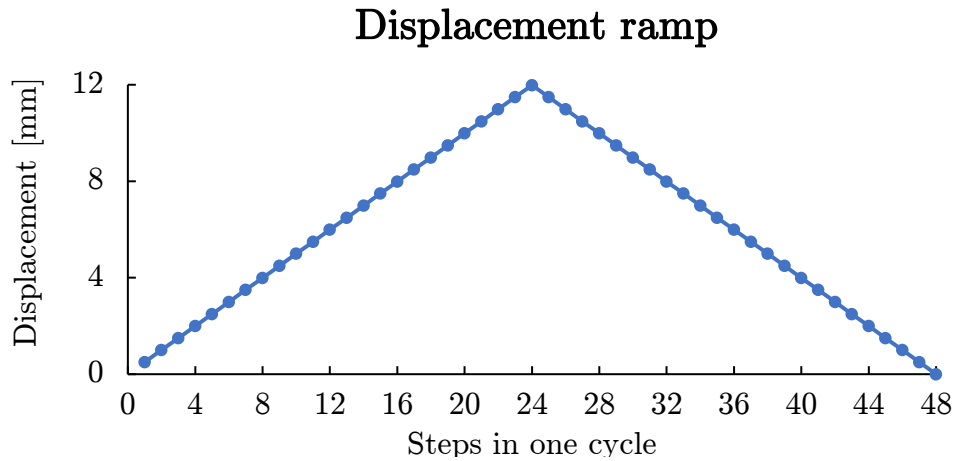
Although the first proof-of-concept of this image-based displacement sensor unit was realized around this personalized framework, the same concept is applicable to any conventional microscope, as shown in the experimental phase presented in *Chapter 3*.

#### **2.1.4 Microscope as a displacement sensor**

As already mentioned, the monitoring system was developed in order to realise a displacement sensor, thus to obtain a single instrumentation capable to analyze the system functioning, while synchronized to other instruments (e.g. encoder on the motor side of the stimulation system). In this way, the image acquisition system can be moved to each well of the functioning bioreactor. The bioreactor platform is capable of reliably follow and monitor each independent culture well with a meaningful advantage in terms of costs.

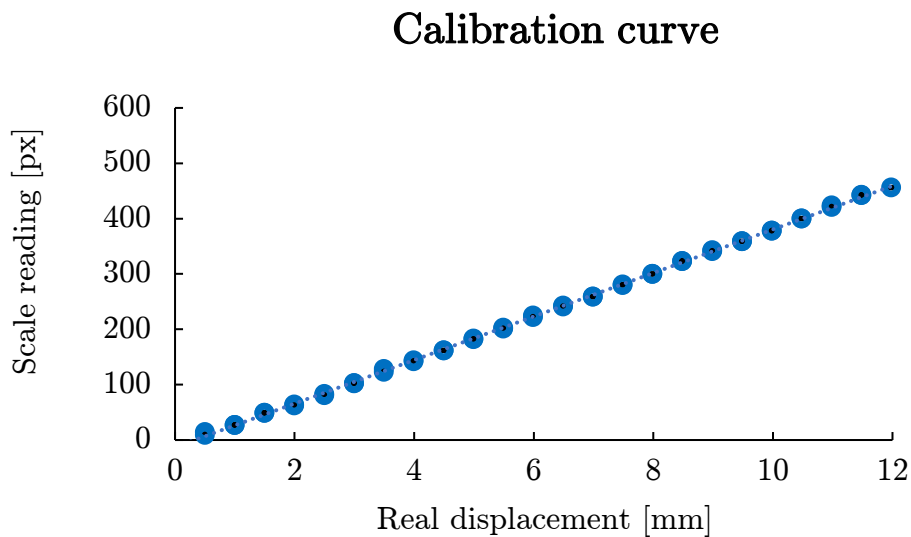
This displacement sensor was calibrated with a standard calibration procedure (*ANSI/ISA-S51.1-1979*) The calibration was done detecting the displacement of a sample (designed similar to the components of the bioreactor to be tracked) that moved along a quasi-static ramp (back and forth) for five complete cycles. As it is shown from the next graph (*Graph*

2.1), each cycle was included by 48 steps, 24 steps in upwards and 24 more downwards, for a total of 12 millimeters displacement.



*Graph 2.1 Displacement ramp of the sample in steps implemented to calibrate the sensor.*

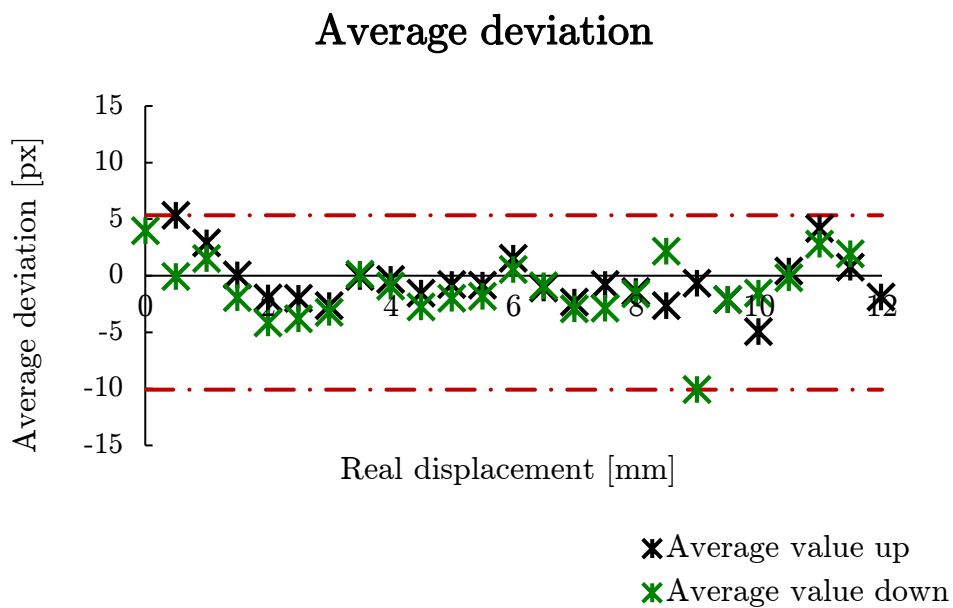
This process provided a set of data as a function of the measurements. Plotting and processing these data, it was possible to obtain the calibration curve (*Graph 2.2*) for different magnifications.



*Graph 2.2 Calibration curve obtained after one cycle of the calibration process.*

To evaluate the sensor functioning and the errors it is better to present the data in the form called deviation plot (reported on the *Graph 2.3*). For each measured value the difference between the measured value (averaging of the measured values of the up-down cycles, reported with the cross markers in black and green color, *Graph 2.3*) and the best-fit equation is calculated (*Wheeler, Ganji, Introduction to Engineering Experiment*). Beginning from the calibration curve, it was calculated the sensitivity value of the sensor.

Using *Graph 2.3*, it was estimated the accuracy of the sensor: all the data are contained between the two horizontal lines in red (parallel to the x-axis) that describe the accuracy interval.




---

*Graph 2.3 Deviation plot: values representing the difference between the measured average value and the best-fit equation is calculated.*

The accuracy interval was calculated for different camera magnification set values and thus different sensitivity values as reported on the following table (*Table 2.1*). The maximum value of sensitivity has been 39.3 pixel per millimetre, while the accuracy includes all residual errors that will occur

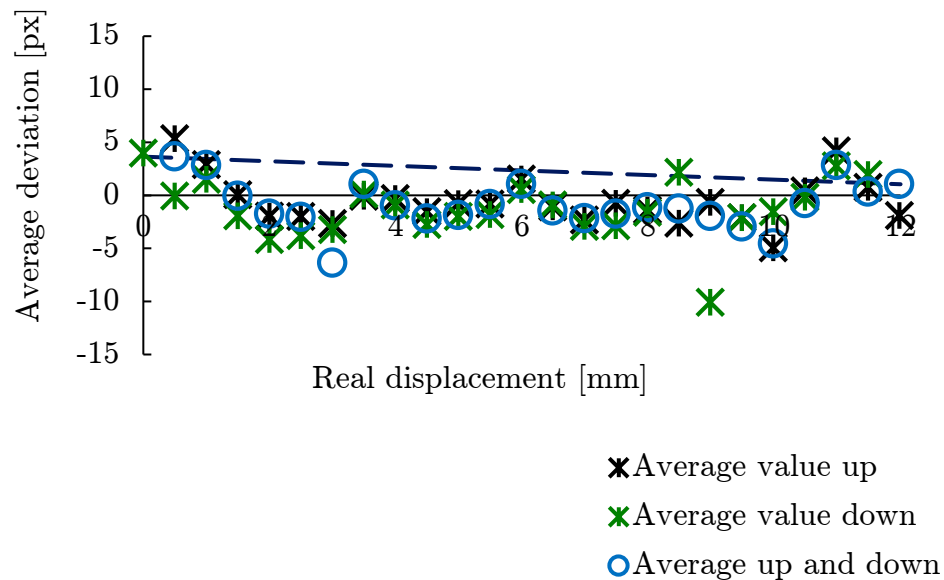
during the sensor using, thus it can be used to estimate the maximum uncertainty in the displacement sensor measurements.

*Table 2.1 Sensitivity and accuracy interval values calculated for different camera magnification.*

Magnification	Sensitivity	Accuracy %
1	39.3 px/mm	-0.9% - 1.7%
2	35.3 px/mm	-0.7% - 0.9%
3	30.9 px/mm	-1.4% - 1.7 %

To evaluate the non-linearity of the data, it was necessary to average the “up” and “down” values measured for each value of real displacement. These data were plotted (*Graph 2.4*) and a line (in blue color) connecting the terminal points of them was drawn.

### Average deviation



*Graph 2.4 Average deviation data for scale calibration.*

## 2.2 BIOREACTOR FUNCTIONING MECHANISM

### 2.2.1 Auxotonic stimulation module

In order to obtain an auxotonic stimulation it is necessary to guarantee a passive loading condition on the construct, implementing a deformable constraint that the maturing contractile tissue is capable of pulling with progressively increasing force. As previously stated, this implementation was realised by the presence of a flexible Nitinol wire, one of the two posts on which the ECT is casted. The longest Nitinol wire is produced by the passive force developed by the neonatal rat cardiomyocytes (NRCM ) embedded on the hydrogel-based tissue.

The deformability of the wire promotes the self-organization and the maturation of the ECT, and measuring the deflection it is possible to implicitly measure the passive force that the construct has been able to produce. The deflection of the beam is indeed directly proportional to the tensile force according to the known Nitinol wire stiffness:

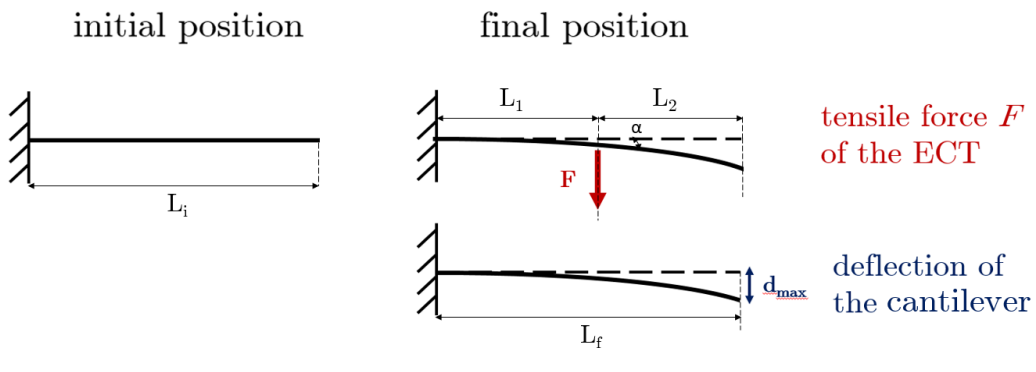
$$Force = k \times d$$

where  $k$  is the stiffness in  $N/mm$  and  $d$  is the measured displacement of the tip of the cantilever, calculated from the deflection of the entire wire, in  $mm$

The use of the longest Nitinol wire was driven:

- a) to easily cast the tissue,
- b) to encourage the development of the construct passive force by applying auxotonic stimulation,
- c) to measure the construct force.

As shown in *Scheme 2.3*, the linear correlation between force and deformation of the cantilever allowed to generate a force transducer precisely locating the ECT with respect to the constraint of the cantilever: an applied force  $F$  by the ECT produces a deflection  $d_{max}$  at the tip of the cantilever. The force was applied on a known distance  $L_1$  from the joint and an angle  $\alpha$  was created between the vertical unload position and the loaded one.



*Scheme 2.3 Cantilever functioning scheme: initial position and final position after the imposing force  $F$  that produces a deflection  $d_{max}$ .*

$d_{max}$  was calculated starting from the linear elastic formulation and it is correlated with the force through the following formula:

$$d_{max} = \frac{F \times l_i^3}{3 \times EJ} + \frac{F \times l_i^2 \times l_f}{2 \times EJ}$$

with:

- $F$  is the applied force (N/mm),
- $l_i$  is the initial length of the cantilever (mm),
- $l_f$  is the length of the cantilever due to the force application (mm),
- $EJ$  is the flexibility module, representing the ability of the beam to resist the deformation in response to an applied force (N x mm).

In detail, the first term of the formulation refers to the length  $L_1$  on which the force  $F$  is applied, while the second term relates to the cantilever deflection of the other end, and to the produced  $d_{\max}$ .

The cantilever was submitted to a distributed load and in order to correlate the deflection to the force measurement, so that to evaluate the contractile force of the ECT, a calibration process of the cantilever was implemented.

### 2.2.1.1 Force sensor calibration

It was implemented a quasi-static calibration process using a tensile force machine (MTS systems). The mentioned machine allowed to impose increasing deflection values to the Nitinol wire with a known varying speed. In details, the cantilever was mounted on the moving extremity of the test machine and pushed against a metal pin with width equal to 3 mm (corresponding to the width of the ECT constructs). The relative motion between the two elements produces an increasing displacement of the wire at the same distance on which the ECT construct would have been positioned. In this way, the calibration procedure assured the mimicking of the tensile force produced by the cells on the cantilever.

The calibration setup (*Figure 2.20*) was mainly constituted by:

- a) suitable 3D printed-frame on which the cantilever was positioned: it was designed in order to offer the same conditions of the bioreactor section on which the cantilever would have been casted,
- b) machine tensile test and relative data processing software,
- c) metal pin mounted to the lower mobile part of the machine.

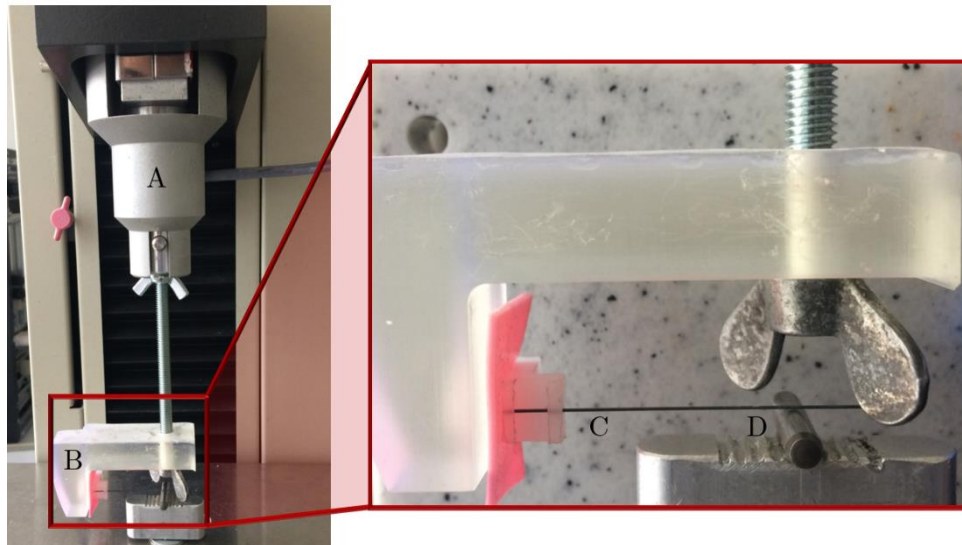


Figure 2.20 Calibration set up: tensile machine test (A), 3D printed-frame (B) for the cantilever (C) embedding, metal pin (D) in zero position.

It was imposed a displacement rate of the pin with a 0.017 mm/s on the direction of the cantilever. Therefore, after a 161 seconds test and a total displacement of 3 millimetres, the Force and then the calibration curve was calculated by the software.

Table 2.2 Calibration test imposed and calculated parameters

	Time [s]	Force [N]	Displ [mm]	Speed [mm/s]
INITIAL VALUE	0	0	0	-0.017
FINAL VALUE	161	0.036	-3	-0.017

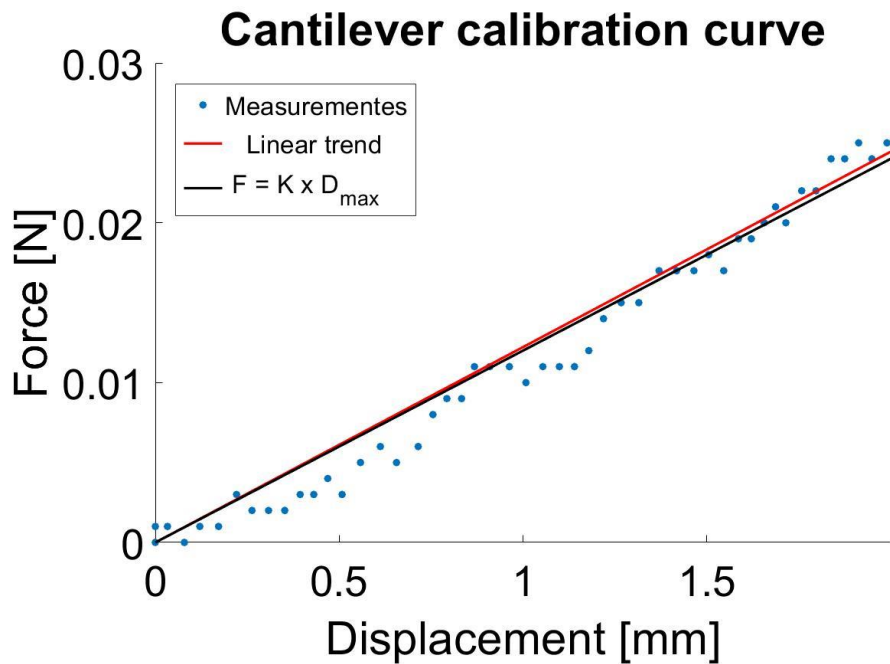
As shown in the *Scheme 2.3*, the calibration was related to the  $d_{\max}$  measurement. Indeed, by measuring that parameter, the obtained value of the sensitivity has been more precise. However, the value that has been

important for the calibration process has been the deflection on the force application point ( $L_1$ , in the *Scheme 2.3*).

As a result, the calibration equation is:

$$F = 0.012 \times d - 0.002$$

with a sensitivity of 12 mN/mm, that represents the cantilever stiffness during the test.



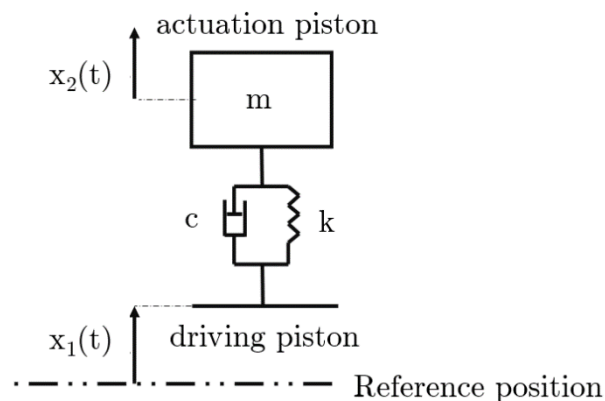
*Graph 2.5 Calibration curve: the force (applied in  $L_1$ ) data (blue) changing the displacement value and the linear trend (red) of the measurement, while the function reported in black color represents the linear elastic formulation, regarding the total length of the cantilever.*

### 2.2.2 Isotonic stimulation module

To apply cyclic loading to the construct, the bioreactor is equipped by a hydraulic system. The actuation system was conceived as a hydraulic syringe-like piston. The idea behind the actuation is a chain of two energy conversions:

- a stepper motor controls the cyclic translation of a driving piston which is moving in a driving syringe,
- the stated piston increases the local pressure of a hydraulic fluid with the consequent generation of a flow rate due to the conversion of the mechanical energy towards hydraulics,
- the flow goes towards a second actuation syringe cylinder where it is converted again into mechanical energy,
- the generated mechanical energy produces the motion of the second piston, which is delivering the movement to the ECTs in the culture chamber.

The use of incompressible fluids in the hydraulic circuit guarantees a stiff transfer of motion from the driving piston to the actuation cylinder. Using water as hydraulic fluid produces the same effect of a high stiffness spring, having a high Bulk modulus . The hydraulic system can be modelled by the lumped approach (*Scheme 2.4*), in which the inertial effects of the moving piston and water mass is concentrated in the lumped mass  $m$ , the spring effect of water is modelled by stiffness  $k$ , and the possible damping given by the viscous dissipation of energy within the tubing and connections is concentrated in the viscous damping factor  $c$ . The model reported in the previous scheme (*Scheme 2.4*) is valid only if the o-ring friction effect of the actuator piston is not considered. In this case, a new suitable model must be designed in order to satisfy the miniaturized size of the hydraulic cylinder.



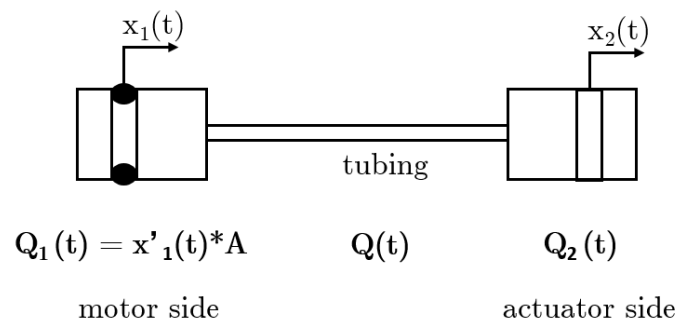

---

*Scheme 2.4 Lumped model scheme of the hydraulic system.*

### 2.2.2.1 Principle of functioning and main components

The displacement  $x_1(t)$  was driven by a motor side. To implement it, a syringe is mounted on a traditional syringe pump that can be easily programmed to produce different flow rate waveforms. The syringe is connected to the actuation side by a semi-rigid transparent tubing. Therefore, syringe, tubing and actuation cylinder constitute the hydraulic circuit in which:

- the pump controls the cyclic translation of the syringe plunger in a waveform (e.g.  $x(t)=A\sin(\omega t)$ ),
- the plunger displacement increases the local pressure of the hydraulic fluid inside the circuit that produces the displacement  $x_2(t)$  on the actuator cylinder.



*Scheme 2.5 Hydraulic circuit representation.  $Q(t)$  is the generated flow rate depending on the section area  $A$ . In the ideal case would be:*

$$Q_1(t) = Q(t) = Q_2(t).$$

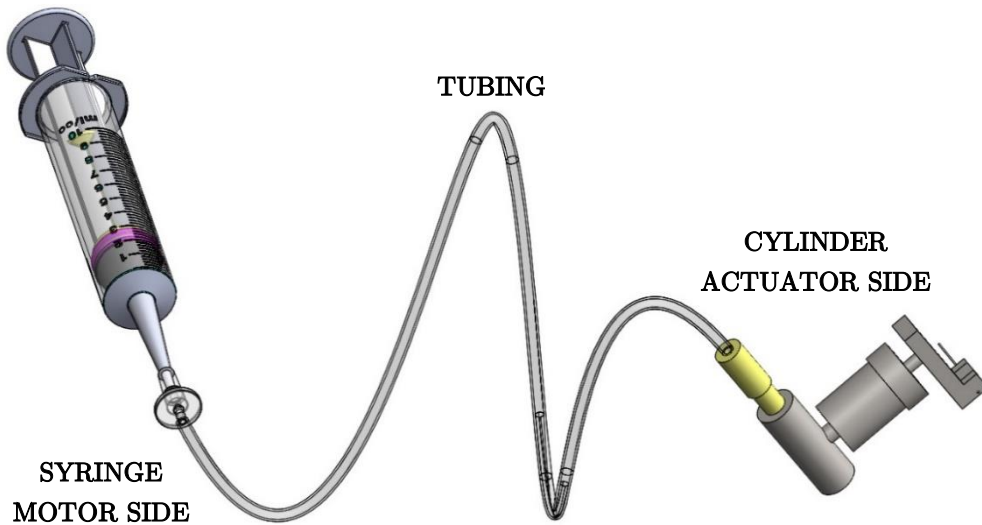


*Figure 2.21 Rendering scheme of the hydraulic circuit: syringe, tubing and actuator cylinder.*

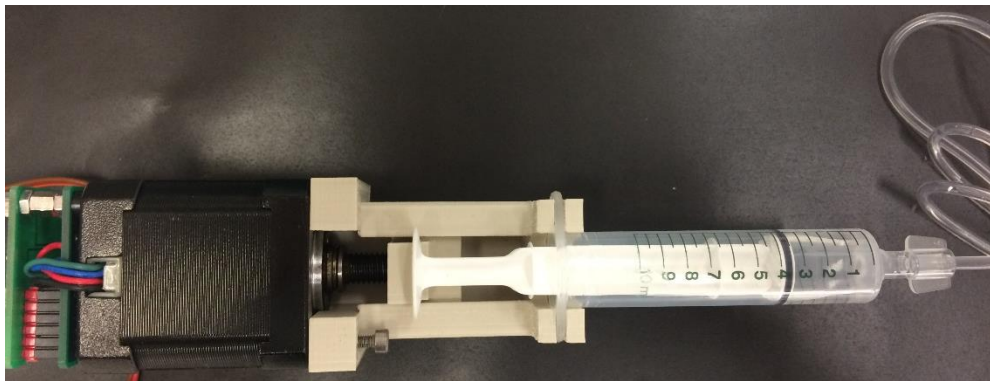


*Figure 2.22 Picture of the implementation of the previous scheme.*

The main advantages to implement a hydraulic system as stimulation module are represented by the possibility to have the the motor and the actuation side far away from each other, giving extreme flexibility to the system. Indeed, there are no rigid connections between motor side and bioreactor instrumentation. The use of an hydraulic system works as a

natural vibration damper, limiting small vibrations delivered to cultured ECTs. Furthermore, these mentioned aspects of the hydraulic module represent essential features to assure to easily work under the microscope systems. In fact, the possibility to drive the bioreactor with just flexible hydraulic tubings allows to avoid bulky kinematics around the microscope lenses, which can result in difficult technical implementation.

#### 2.2.2.1.1 Portable syringe pump device

As an effective alternative to the traditional syringe pumps, it was developed another design for a moving and portable syringe pump (*Figure 2.23 -2.24*). It was simply constituted by a suitable syringe adaptor and a stepper motor apparatus that drives the syringe displacement.

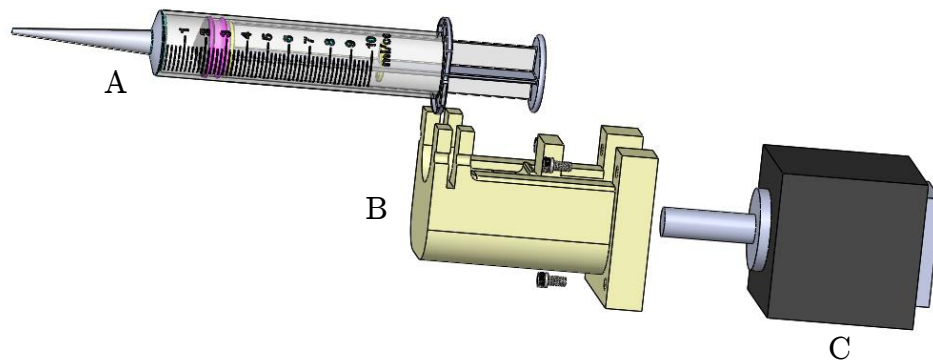


*Figure 2.23 Rendering of a Solidwork exploded view of the portable syringe pump device. Syringe (A), syringe adaptor (B) and motor side (C).*

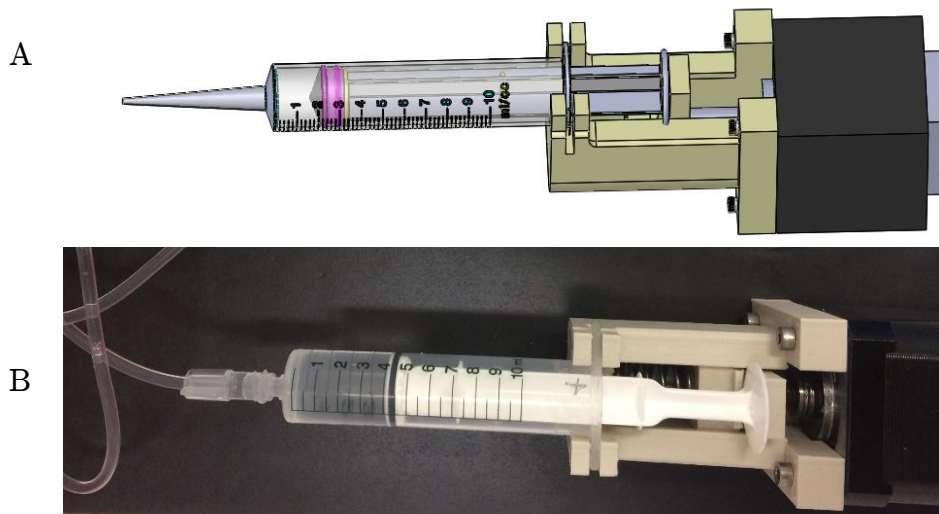


Figure 2.24 Solidwork assembly of the device model (A) and picture of the designed device (B).

The motor was implemented to play the syringe pump engine role, directing the cyclic translation of a syringe piston (e.g. sinewave form  $x(t)=A\sin(\omega t)$ ). The stepper motor principle of functioning was inspired by the 3D printers functioning: the cyclic displacements back and forth was produced thanks to a combination of a real motor ( $x$ ) and a virtual motor ( $y$ ). In this way, a virtual circle (Figure 2.25) can be obtained and the latter can be decomposed as combination of:

$$\begin{cases} x = R \cdot \cos \theta \\ y = R \cdot \sin \theta \end{cases}$$

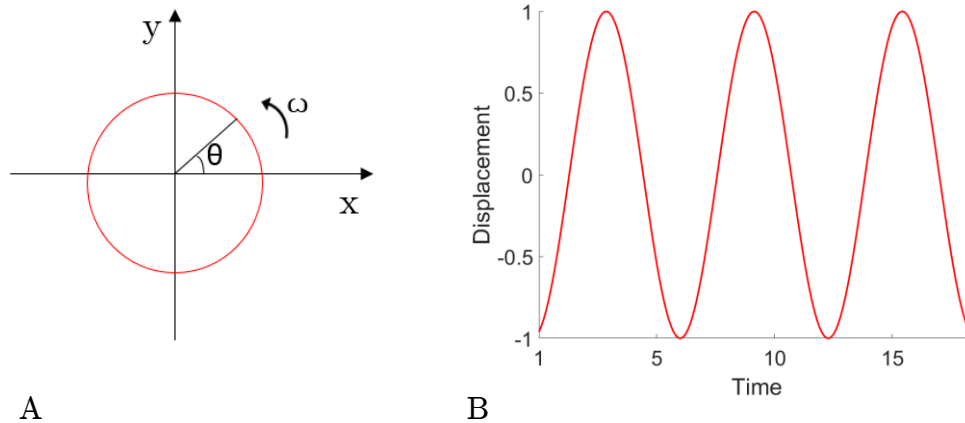


Figure 2.25 Virtual circle defined by the motor engine (A) and linear displacement derived from that (B).

Therefore, the operating mechanism of the motor could generate a rotation with radius  $R$  and angle  $\theta$  that was then translated in a linear displacement (Figure 2.25 (B)). It was implemented exploiting the already existing *Bresenham algorithm* regarding the generation of circle over the plane that allowed to impose a sinewave  $x(t)$ . Since the round shape can be decomposed as sine and cosine functions over the plane x-y, the efficacy of this solution was to have a real motor and a virtual one that were able to generate circles defined by a radius that is equivalent to the stretching length during the mechanical stimulation and by the angular velocity related with the frequency of the cyclic loading on the tissue.

To set the cyclic transition parameters, the stepper motor was controlled by a microprocessor that communicates with a serial adaptor. The latest is connected to the computer through an USB port and it can be controlled by a Matlab code that was allowed:

- a) to recognize the connected serial adaptor,
- b) to start the motor functioning,
- c) to set up the main functioning parameters,
- d) to stop it.

The Matlab script was indeed used to impose the operating parameters of the mechanical stimulation:

- a) the step dimension ( $S$ ) related with the stretching length,
- b) and the frequency ( $F$ ).

The described tool has led to the advantage to be able to program the engine to generate different waveforms for the fluid displacement, thus for the mechanical loading protocols, using the Matlab code. Moreover, it has guaranteed an effective usability especially to easily move the stimulation module in different positions without space problems, the obtention of an independent instrumentation.

#### **2.2.2.2 Hydraulic system filling procedure**

The hydraulic fluid chosen to fill the module has been the distilled water.

Air bubble nucleation inside the hydraulic circuit could represent one of the main issues related to the use of a mechanical system like the described one. The stiffness dominant behaviour of the system could indeed be modified by the possible presence of air bubbles. Since air is a compressible fluid, it could have a compliance effect in the circuit energy transfer and thus in the efficiency of the hydraulic circuit functioning.

In order to try to reduce as much as possible the presence of air, it was implemented and then applied a precise filling procedure of the system summarized on the *Scheme 2.6*. The core materials that have been used are:

- a) distilled water,
- b) vacuum pump,
- c) tube, syringes and 3-ways stopcock.

And the procedure was constituted by three different stages, schematized on the *Scheme 2.6*.

### First stage:

The first stage was essential to obtain a degassed hydraulic fluid allowing to reduce the probability to induce air bubble creation during the filling procedure. In fact, a tube of distilled water was connected with a high vacuum pump that in around five minutes produces a degassed fluid. In order to monitor the level of vacuum generated, the latest was also associated with a manometer (*Figure 2.26*).

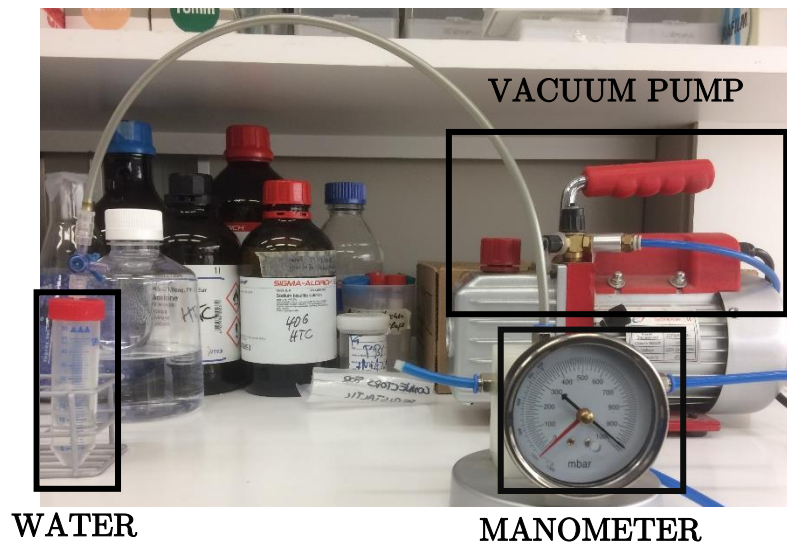


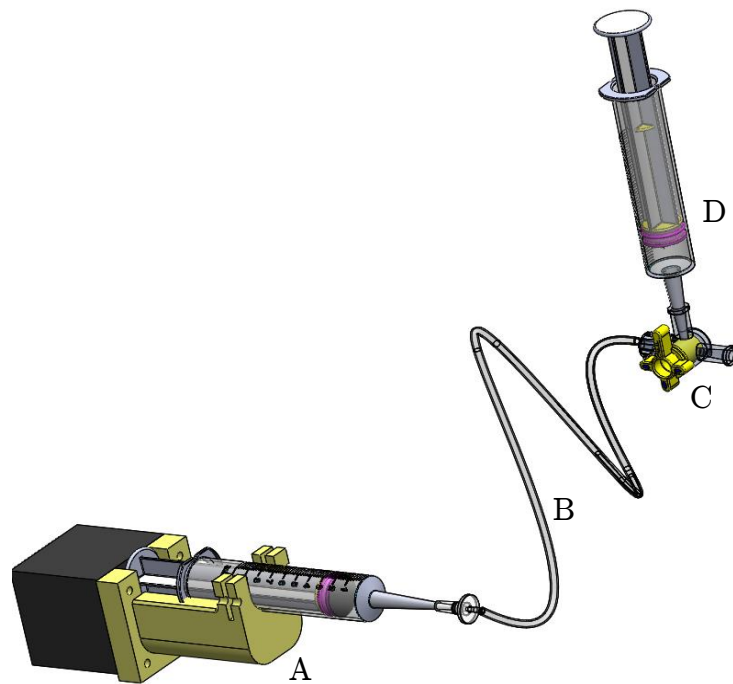
*Figure 2.26* Picture of the main elements exploited in the first stage of the filling procedure.

### Second stage:

The same instrumentation was used to create the vacuum into the first portion of the hydraulic circuit: syringe (engine side) and tubing. Therefore, the tubing already mounted with the syringe were connected to the vacuum pump and the actuation of it was generated an under vacuum circuit.

### Third stage:

The degassed water in a syringe is connected to the tube using a 3-ways stopcock. The vacuum previously created inside the circuit allows the filling process since, opening the communicating way between the degassed water syringe and the tubing, the fluid is sucked into the vacuum.



---

*Figure 2.27 Rendering scheme of the third stage of the procedure: portable syringe pump (A) together with the tubing (B) of the implementing hydraulic circuit connected through a 3-ways stopcock (C) to the degassed filling fluid.*

After the filling of the first part of the circuit, it has been necessary to connect the actuation side of it. Therefore:

- the cylinder element is connected to the filled tubing,
- the fluid is pushed through the syringe plunger pressing up to reach the hollow part of the actuator cylinder,
- the previous step also assures the spillage of eventual low density air bubbles,

- the piston element of the actuator was positioned in the upper part of the open cylinder,
- pulling on the fluid thanks to the depression creates moving away the syringe plunger, the piston was pulled inside the cylinder.

In this way it was possible to obtain a filled and closed hydraulics circuit.

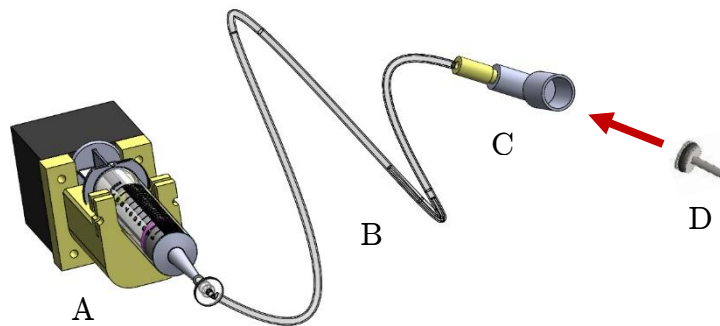
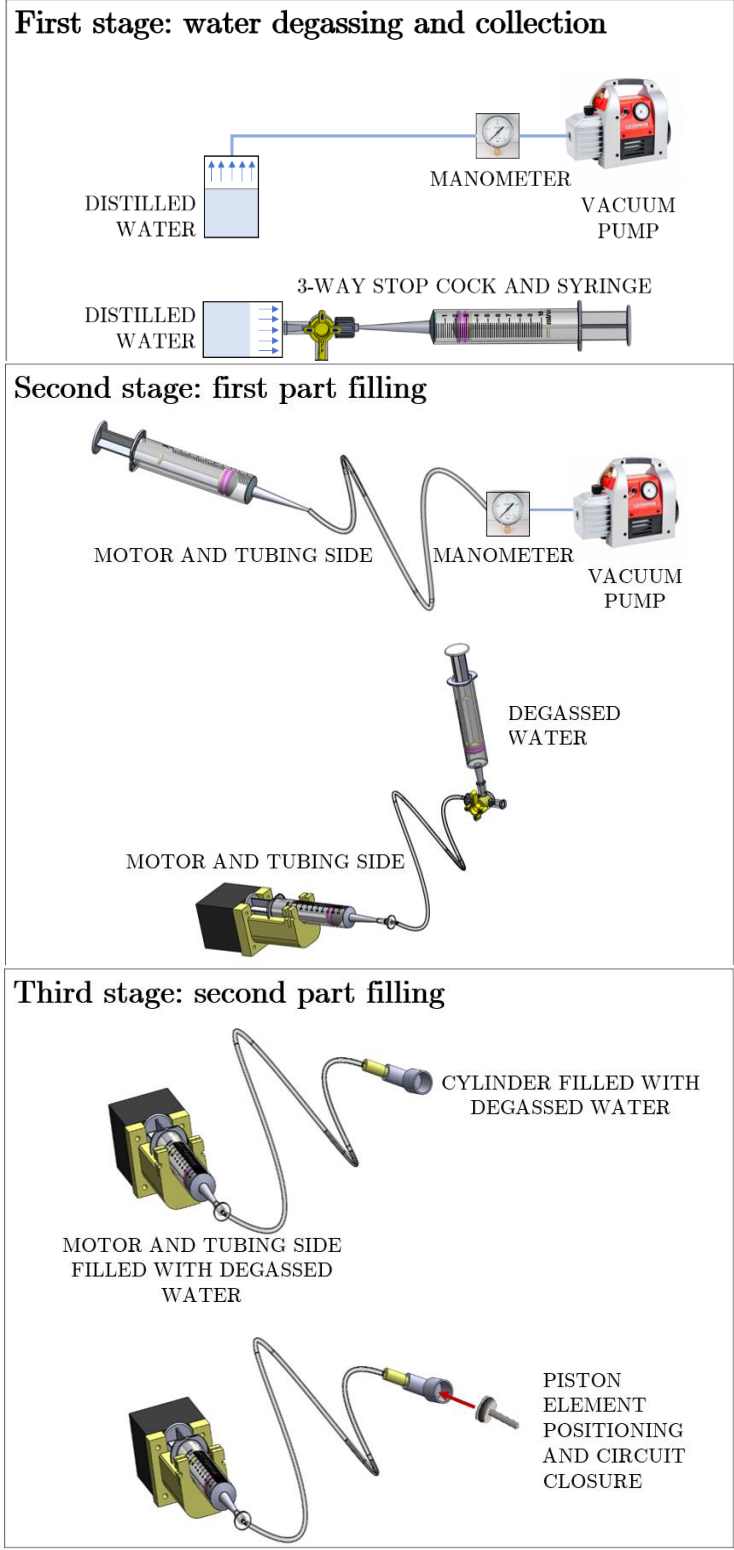


*Figure 2.28 Rendering scheme of the fourth stage of the procedure: syringe pump (A) together with the tubing (B) connected to the cylinder actuator (C) and, through the previously described technique, piston inclusion on the circuit (D).*



*Scheme 2.6 Schematic representation of the filling procedure stages.*

### 2.2.2.3 Characterization of the mechanical stimulation system

To characterize in the best way the operating mechanism of the hydraulic system, it has been necessary to detect and to analyse the movement of the actuator piston, carried out by the engine. The study was conducted through the acquisition of videos. The videos were recorded exploiting the monitoring unit described in the dedicated sub-chapter (2.1.3). As previously mentioned, this unit was implemented and then calibrated in order to work as a displacement sensor. Therefore, the sensor has played a fundamental role on the characterization of the dynamic stimulation module: the camera, connected to the computer, follows the cyclic transition of the clamp mounted on the actuator piston and it has been useful to analyse the waveform imposed by the driving piston during the biomechanical stimulation of the ECT. The camera recorded video was automatically saved and then it was appropriately elaborated implementing the segmentation routine previously defined (*Scheme 2.2, Figure 2.19*). Consequently, as it was partially explained in the 2.1.4 section, the monitoring unit acquisitions were used to extract the main parameters of the waveform described during the cyclic translation of the piston. The parameter analysis has been optimized thanks to the values obtained from the calibration of the monitoring unit (referring to the results reported on the *Graphs* from 2.1 to 2.4).

The displacement waveform was initially set as a sinewave form, but correspondingly rectangular or triangular waveforms could be implemented. The parameter extraction of the imposed translation was made easier thanks to the image processing routine. With a great resolution, the microscope lens was focused on the upper part of the with clamp (*Figure 2.19 (B, C)*) driven by the piston and in this way, they could follow the displacement of the centre mass of the followed sample, as it has been summarized by the following scheme (*Figure 2.28*). Therefore, the acquisition system was connected to the computer by an USB port and the functioning was monitored through Matlab code that allows:

- a) to set the communication with the camera;

- b) to set the main acquisition parameters;
- c) to have a preview of the recording field;
- d) to start the video acquisition of the piston's displacement, following the clamp back and forth translation (*Figure 2.17 (B, C)*);
- e) to elaborate the recorded video (*Figure 2.17 (D)*);
- f) to extract the waveform of the piston displacement, saving the main parameters, in order to evaluate if the imposed waveform translation was preserved (*Figure 2.18*);
- g) to calculate the waveform Fast Fourier Transform (FFT).

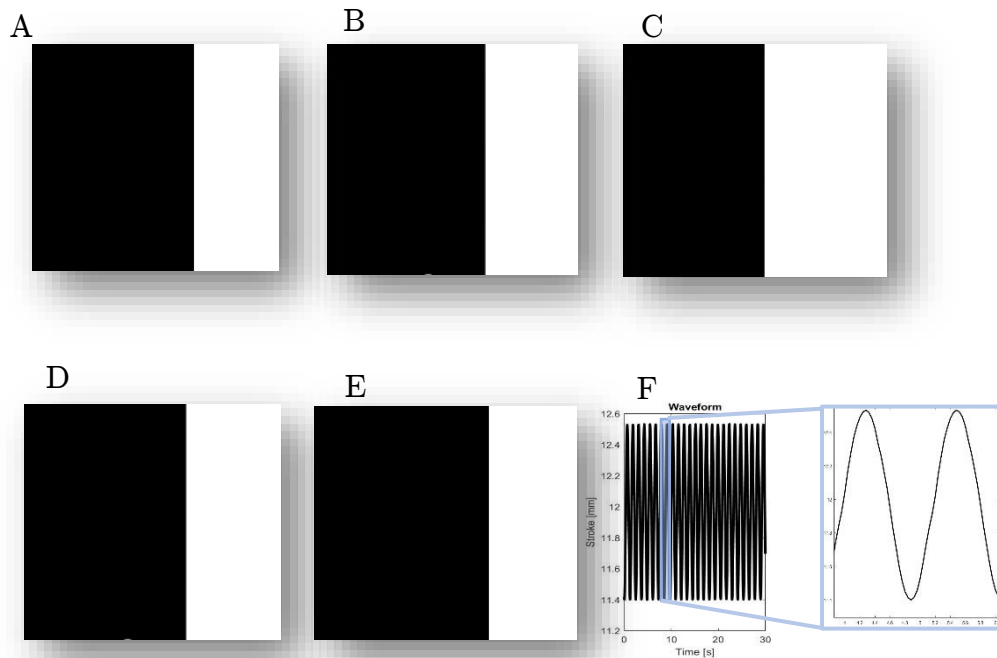


*Figure 2.28 Examples of photoshoot from the segmented video over the cyclic sinewave translation (A-E); example of sinewave parameter extraction (F).*

In order to characterize the main features of the hydraulic system functioning, but also to evaluate the stability over the time and the eventual issues of it, several tests were implemented.

#### **2.2.2.3.1 Static condition checking**

Initially, the piston position was evaluated in static condition in order to estimate the stability over the time of the system. To implement the static tests the initial position was documented by the camera (defining the test starting) and the second acquisition of the position was recorded after 16 hours (test ending). In this way it has been possible to verify potential changing on the system.

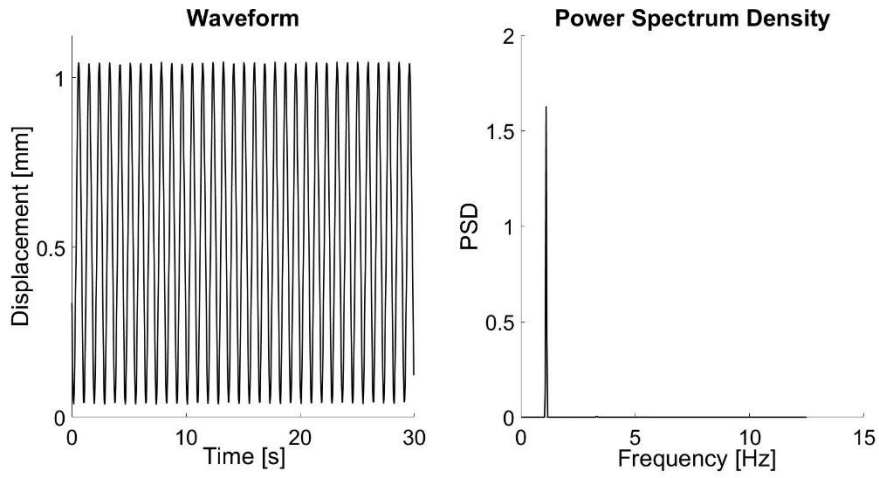
#### **2.2.2.3.2 Dynamic condition checking**

Regarding the dynamic condition study of the system, the principle of the monitoring unit use has been equal. In detail, the motor side was programmed to generate sinewave forms defined by different parameters. Therefore, changing the amplitude and the frequency values, different functioning has been considered and the features of that functioning have been extracted using the Matlab routine (*Figure 2.18*).

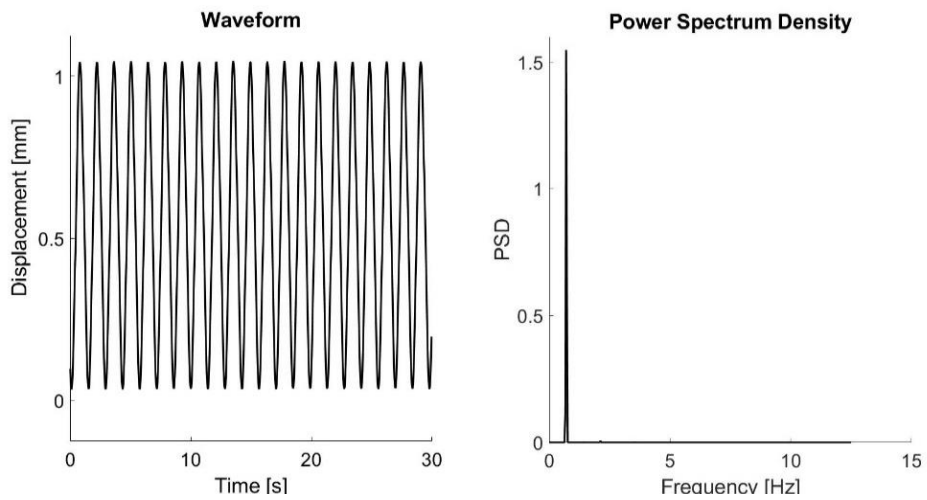
The stated routine allowed to assess if the sinewave generated by the motor side was effectively preserved on the actuation side. In fact, the calculated parameters have provided the real waveform that is the one that has been used to generate a cyclic stretching of the tissue. Using the same Matlab functions, it has also been possible to compare the obtained sinewave with the real one characterized by the same parameters.

#### **2.2.2.3.3 Characterization results**

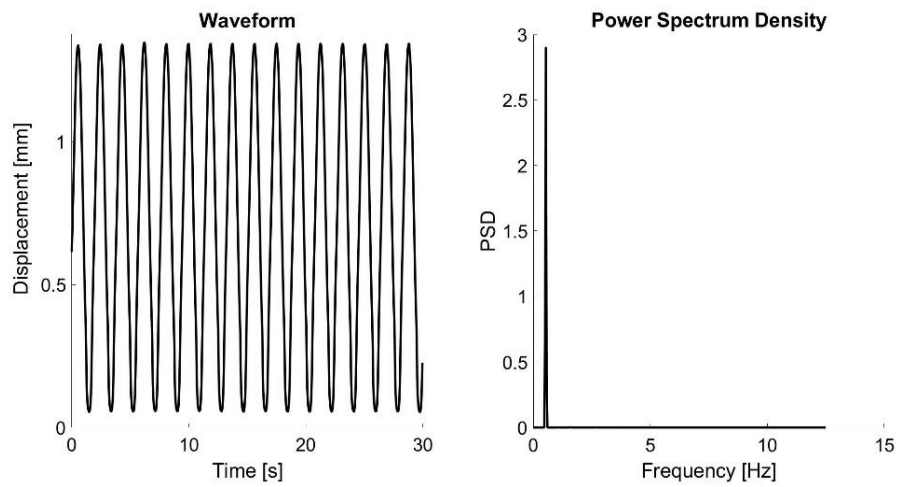
The dynamic tests have shown that the set displacement waveform was preserved on the actuation and that they were stable over the time:



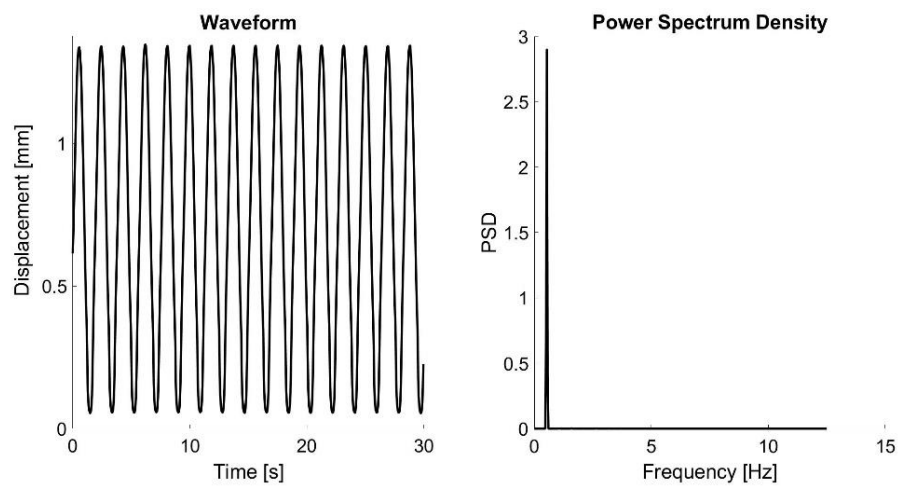
*Graph 2.6 Example of waveform and FFT detection of a 30 seconds translation of the actuation piston (displacement 1 millimetres and frequency 0.8 Hz).*



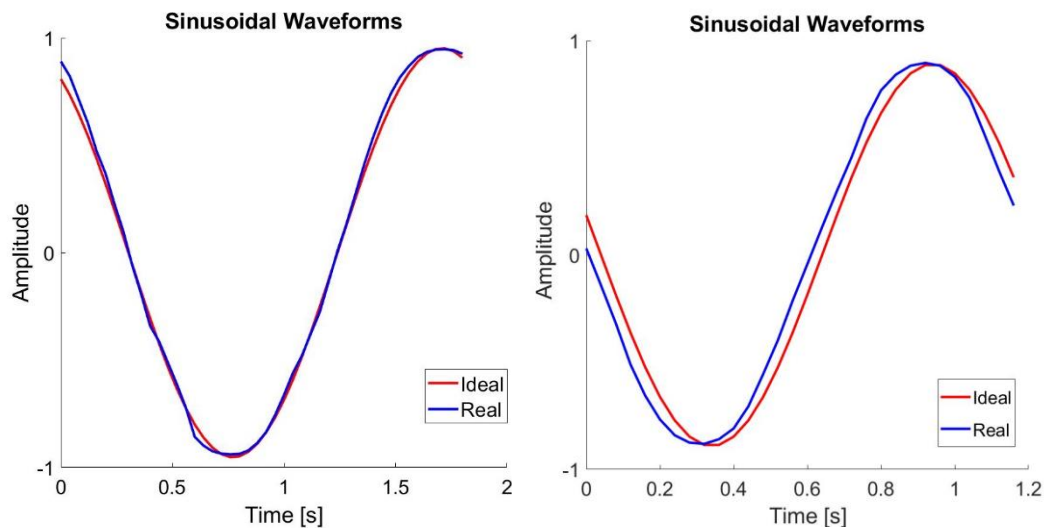
*Graph 2.7 Example of waveform and FFT detection of a 30 seconds translation of the actuation piston (displacement 1 millimetres and frequency 0.56 Hz).*



*Graph 2.8 Example of waveform and FFT detection of a 30 seconds translation of the actuation piston (displacement 1.5 millimetres and frequency 0.56 Hz).*



*Graph 2.9 Example of waveform and FFT detection of a 30 seconds translation of the actuation piston (displacement 1.5 millimetres and frequency 0.56 Hz).*



*Graph 2.10 Example of waveform comparison between imposed and ideal sinewave (displacement 1 millimetres and frequency 0.56 Hz (A) and 0.8 Hz (B)).*

The initial tests, both in static and in dynamic condition, have shown the presence of a drift error. This error was monitored both in static and cyclic functioning, but also checking the changing on the average value of the sinewave during dynamic tests.

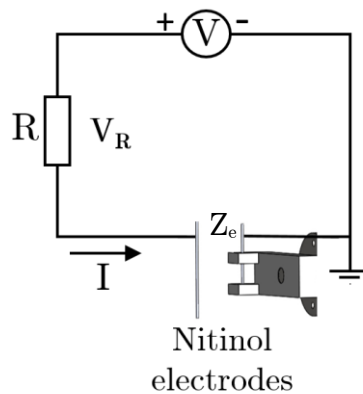
The results were comparable and not markedly different, both in dynamic and static conditions. Afterwards, it was demonstrated that the drift error was linked to some leakages of the hydraulic circuit. With an optimization of the filling procedure of the system, together with the use of lubricant on the more critical components (actuator piston and syringe plunger), the drift error was reduced to be irrelevant on the stimulation module functioning.

### 2.2.3 Electrical stimulation module

The contractile functionality of the ECT could be evaluated monitoring spontaneous and electrically paced beatings.

To implement the electrical stimulation, the Nitinol wires were exploited as electrodes connecting them to an electrical pacemaker, it allowed to impose different impulse values. The heart construct, is casted between the Nitinol posts and the electrical terminals and can be coupled to them in order to provide electrical stimuli to the tissue.

The electrical scheme of the described system is the following:



*Scheme 2.7 Electrical circuit scheme: between the two electrodes (impedance  $Z_e$ ) the ECT is embedded; the imposed voltage  $V$  generated a current  $I$  through the resistance  $R$ . The current  $I$  is the current on which the construct is exposed.*

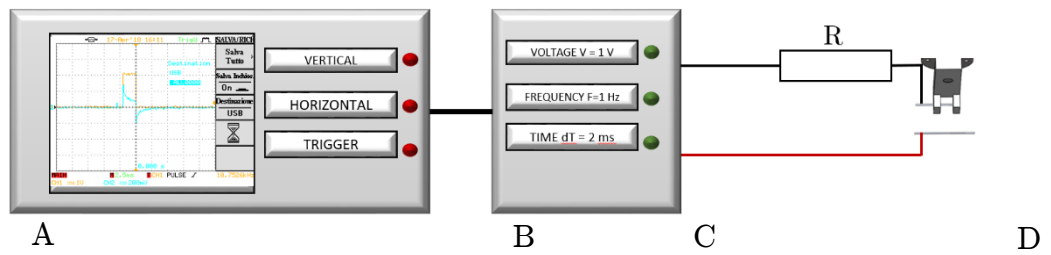
During the electrical pacing of the construct the temperature must be kept constant at 37°C and it is placed between the Nitinol electrodes, covered by the culture medium. The latest has electrochemical properties that contribute to generate an electrochemical cell functioning.

### 2.2.3.1 Characterization of the electrical circuit parameters

To measure the main parameters of the described electrical system, it was executed a calibration process of it. The procedure was based on the measurement of the current resulted by imposing precise voltage pulses.

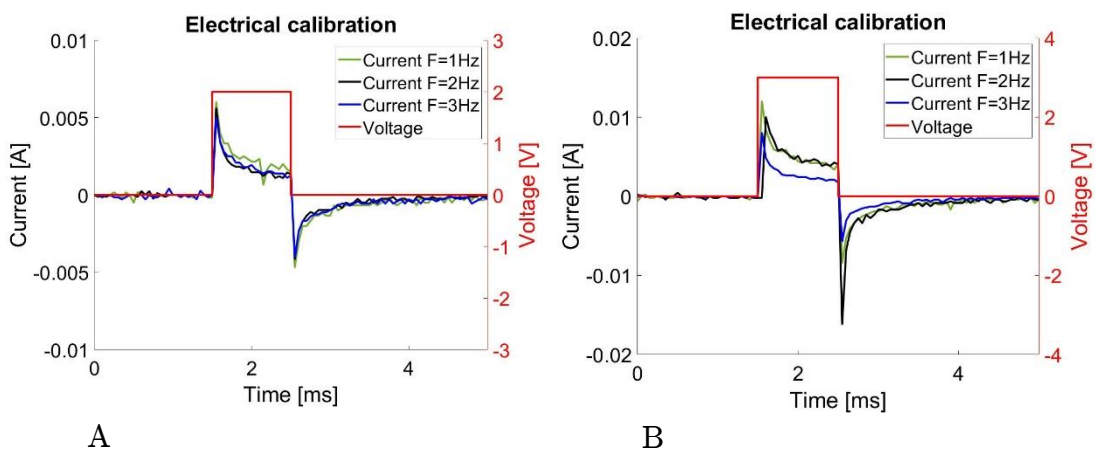
The characterization process (*Scheme 2.8*) was implemented using the following set up:

- a) oscilloscope for the current measurement,
- b) electrical stimulator for the pulse generation,
- c) Nitinol electrodes of the device.

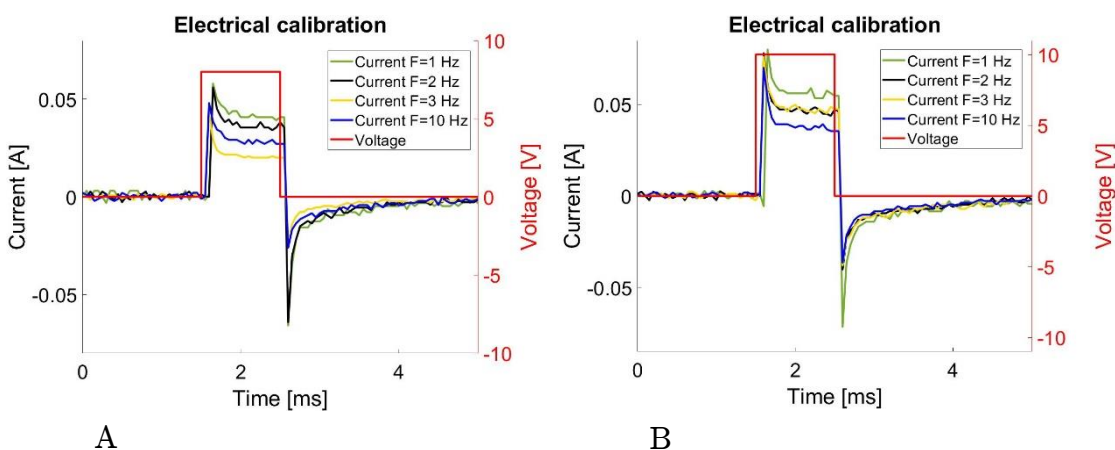


*Scheme 2.8 Electrical calibration set up: oscilloscope (A), pulse generator (B) connected with the electrical terminals (C) to the electrodes of the system (D) through a resistance R.*

Through the described setup, rectangular-shape pulses at different values of voltage (from 1 Volt to 10 Volts) and at different frequencies ( $F = 1, 2, 3, 10$  Hz) with a duration of 2 milliseconds, were imposed. For each pulse generation, the charge injection measurement, thus the circuit current, was acquired and saved.



Graph 2.11 Examples of electrical calibration result: measured current with a pulse of  $V=2V$ ,  $F=1-2-3Hz$ ,  $dT=2ms$  (A) and with a pulse of  $V=3V$ ,  $F=1-2-3-10Hz$ ,  $dT=2ms$  (B).



Graph 2.12 Examples of electrical calibration result: measured current with a pulse of  $V=8V$ ,  $F=1-2-3-10Hz$ ,  $dT=2ms$  (A) and with a pulse of  $V=10V$ ,  $F=1-2-3-10Hz$ ,  $dT=2ms$  (B).

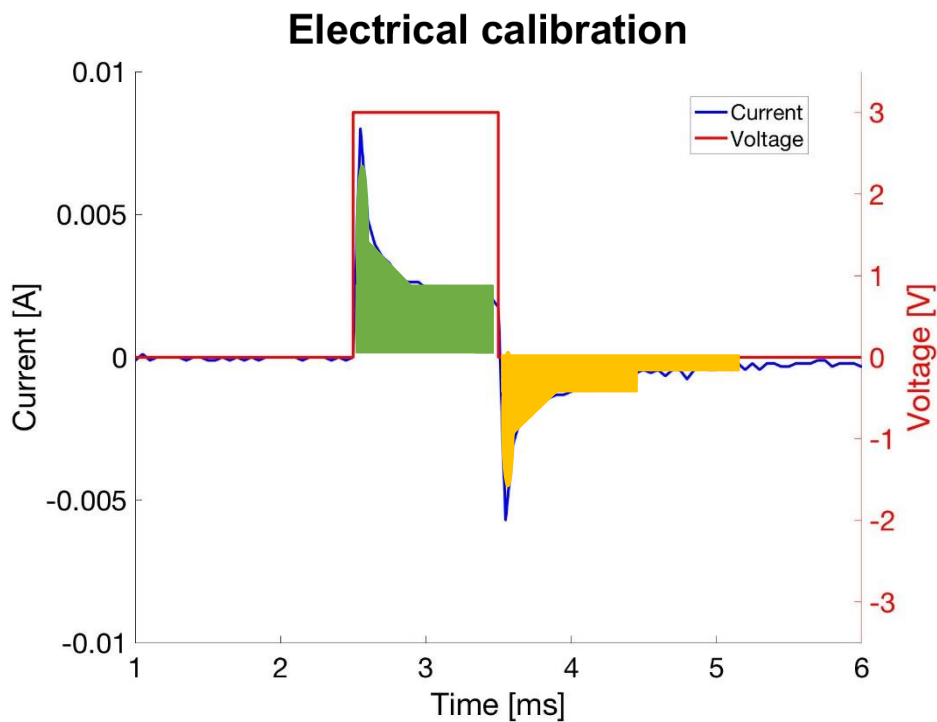
In the describing circuit, the charge transfer could occur through three different mechanisms:

- a) non-faradaic charging/discharging,
- b) reversible faradaic reaction,

c) non-reversible faradaic reaction (*Tandon, et al. 2006*).

Since the ECT is in the culture medium in which the charge is carried by the ions, the movement of the ions determines the transient presence of current in the system. That current is produced by the electrical field to which the tissue is exposed.

As the previous graphs shown (*Graph 2.11-2.12*), the main charge transfer mechanism is the non-faradaic charging/discharging, since the injected charge is almost totally recovered. That balance between the injected and the recovered charge means that the electrical stimuli do not produce by-products that could be toxic for the tissue.



*Graph 2.13 Example of electrical calibration result: measured current with a pulse of  $V=3V$ ,  $F=1Hz$ ,  $dT=2ms$  with the detail of the total area representing the injected (in green) and recovered charge (in yellow) during the stimulation.*

Moreover, the results of the electrical characterization revealed that both in charge injection phase and in recovered charge phase, after a quick transient spike the current remains constant.

# 3 EFFECTS OF COMBINATION OF AUXOTONIC AND ISOTONIC MECHANICAL STIMULATION ON MATURATION AND CONTRACTILE PROPERTIES OF ENGINEERED CARDIAC TISSUE – A PROOF OF CONCEPT

---

## 3.1 INTRODUCTION

In the past years, several techniques allowing neonatal rat cardiomyocytes to generate an in vitro contractile 3D engineered cardiac tissue were presented. The main aim of these approaches is to establish a suitable cell culture environment clues for the cells resembling a uniform cell distribution, growing and self-organization (*Jakab, et al. 2010*). The materials used to obtain such a tissue must be:

- a) non toxic for the cell structures,
- b) non inflammatory inductive,
- c) balanced inclined to the degradation (*Ye, et al. 2000*).

To maintain 3D structures in engineered tissues, the currently used materials are either artificial polymers (e.g. polyglycolic acid, polyhydroxy butyrate) or biological gels such as collagen (*Ye, et al. 2000*). For example, in 1999 the Eshenhagen's research group has presented a method that allows NRCM to create a spontaneously beating 3D engineered cardiac tissue, using Velcro-coated silicone matrix (*Zimmermann, et al. 2000*). Furthermore, similar procedures were published during the following decade, since also liquid matrix based on rat tail collagen was used (*Kensah, et al. 2011*). However, the exploitation of these materials leads to the obtention of a tissue with properties still far from the ideal, combined with a high price of the necessary compounds to obtain it (*Ye, et al. 2000*).

Consequently, since it has become evident that the cell culture conditions could have a strong impact on the NCRMs evolving in studies regarding in vitro models, a hydrogel-based approach was implemented. As demonstrated by Haiguang Zhao and colleagues, the use of hydrogels in the CTE context could create great biomimetic conditions for the cells environment (*Zhao, et al. 2008*). They were focused on the fibrin gel optimization and fabrication, aiming to understand the importance of the gelation condition and the influence of the compounds on the degradation temperature.

Therefore, in this thesis project, the fibrin gel production technique was exploited to generate a cardiac tissue.

To develop a biomimetic environment, the native-like tissue conditions is not enough. Indeed, that milieu should be able to provide the cells with the factors that govern the in vivo process (*Jakab, et al. 2010*). Regarding the delivering of physical stimuli, bioreactor approach is essential. Moreover, the cardiac construct properly positioned inside that tool could provide different stimulation condition, helping the tissue maturation. Even in this field, different approaches were offered. The ECTs are usually blocked by an element that either avoid the migration of it both mimicking the bio stimuli. In this study, the (ECT) was casted between two Nitinol wires, as previously stated, and both provide the mechanical stimulation with two different strategies.

The in vitro model must be properly analysed in order to characterize and to measure the biological response due to the set conditions. In detail, the experiment was planned in order to estimate the effects of the combination of the auxotonic and isotonic mechanical stimulation on the maturation of ECTs. Therefore, at the end of the culture, the construct was analysed through:

- a) external electrical pacing,
- b) histological evaluation.

The electrical stimulation represents one of the previously described modules of the bioreactor device. For the moment, the pacing was conceived as an end-point functional test, to evaluate the contractile force and functionality developed during the culture and the stimulation environment. However, in principle electrical stimulation could be executed on the tissue during the culture period .

Regarding the histological analysis, they allow to evaluate which are the structures involved on the tissue maturation, how they expressed and how they are organized relating with the fibrin milieu. Two different techniques were implemented to obtain histological results:

- a) immuno-histochemical,
- b) immunofluorescence.

Through the first approach, it was possible to evaluate the cells organization, their structures and their relationships with the fibrin element. Moreover, the use of immunofluorescence provides the characterization of the cells involved and the main functionalities that they could develop.

## **3.2 MATERIAL AND METHODS**

The principle of functioning of the miniaturized microscope-based bioreactor (described in the previous chapter) was exploited to implement a proof of concept. The biological experiment was realized using a new design version of the bioreactor. While the mechanical and electrical characterization were easily implemented, for the first device test a more compact and usable version was necessary.

### Miniaturized microscope-integrated bioreactor: $\beta$ -version

The main advantage of the new design (*Figure 3.1*) is the compactness and the easily production: one single piece was included between the two components of a 20 cm<sup>2</sup> culture area Petri dish, thus between the bottom and the lid of the culture dish. The prototype was manufactured by a PLA based 3D printer (*MakerBot Replicator +*) and the CAD model (*SolidWorks*) was realized to implement basically a spacer fitting between the dish elements and to guarantee the mechanical stimulation modules inclusion.

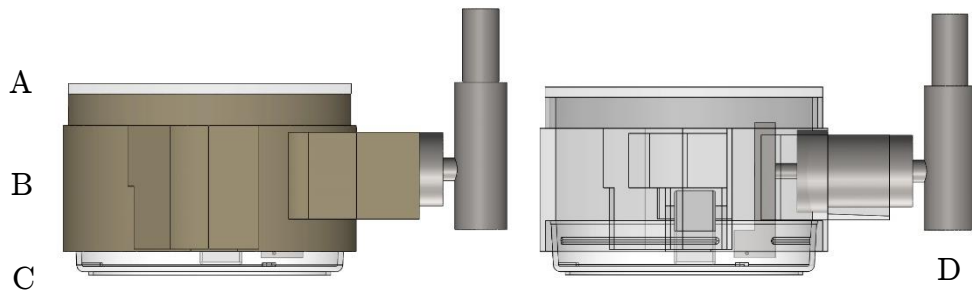


*Figure 3.1 Solidworks rendering of the beta-version design. On the left, the three main compounds are visible: Petri dish lid (A), 3D printed-spacer frame (B) and Petri dish bottom part (C). The same rendering is presented on the right with a transparency view of the frame that makes easier to understand the mechanical stimulation module (D) inclusion on it.*

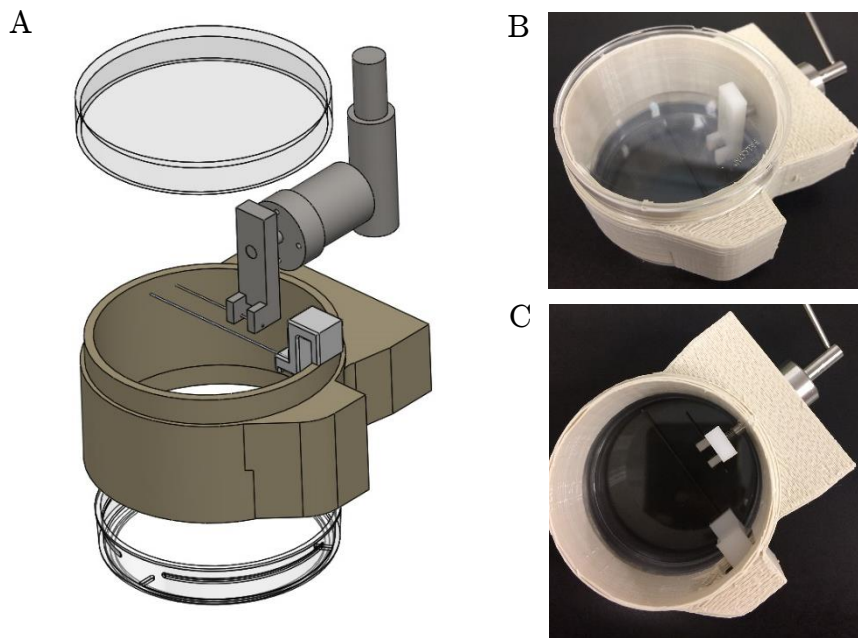


*Figure 3.2 Solidwork exploded view of the device assembly (A) and device assembly pictures (B,C).*

The characterization of the functioning modules of the device (auxotonic and isotonic stimulation module and electrical stimulation one) is valid and effectively reliable also in this version of the bioreactor. One of the main features that make unique the device is indeed the great opportunity to change the frame design, keeping the previous characterization of the device. In this way, the core of this tool is represented by its modules (actuation, force transducer module), since they can be organized in different design versions without altering the functionality of the device.

The described beta-version bioreactor has been tested in order to perform an in vitro three-dimensional ECT, applying cyclical mechanical stimulation. As mentioned in the introduction of the manuscript, the idea behind the construct realization was based on the use of a hydrogel, in order to obtain a fibrin-based heart tissue. The hydrogel generation was driven by the neonatal rat cardiomyocytes (NRCM) embedding on it. First, the experiment was planned in order to gain three replicates in different conditions:

- a) construct kept in static condition in a normal culture dish, without any kind of stimulation, as a control,
- b) construct subject to auxotonic stimulation,
- c) mechanically stimulated construct with a combination of auxotonic and isotonic conditions.

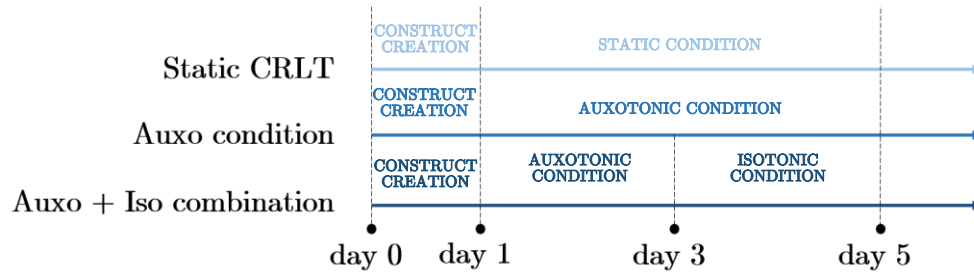
As the graphic experiment plan summarized (*Scheme 3.1, 3.2*), after the cardiac construct generation:

- a) the static replicate was kept in culture for 5 days,
- b) the first actuated replicate was cultured in auxotonic condition, thus without externally controlled dynamic stimulation, for 5 days, with the promising environment to assure the maturation,
- c) the third condition was cultured for 3 days in auxotonic condition, then by applying a cyclic isotonic stimulation for additional 2 days.

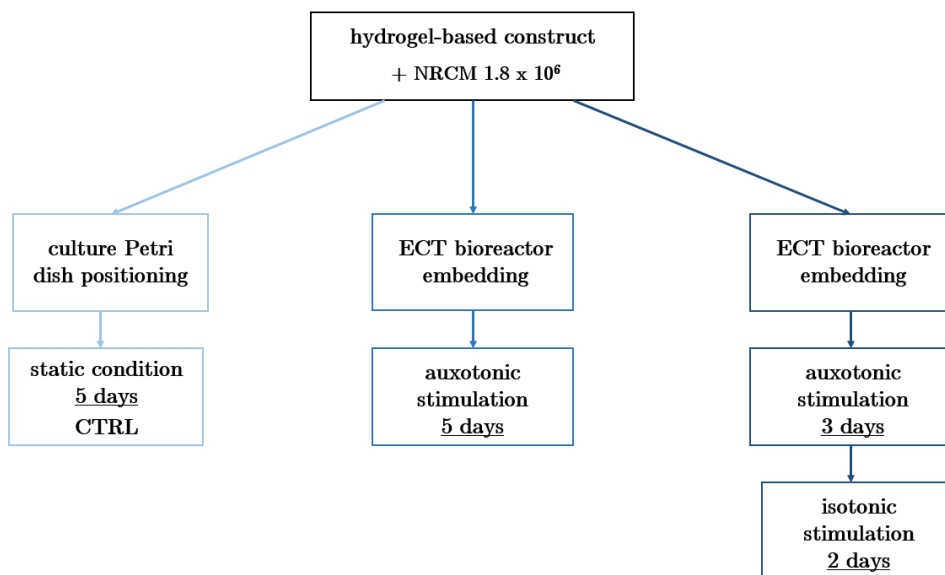
The parameters that have characterized the dynamic loading were set to apply 10% physiological strain and 1 Hz frequency of it.

The cardiac cells embedded in the engineered tissue were passage zero cells, used after 5 days from the isolation process. During the first 2 days experiment, the culture medium suspension was added with 1.5 TIU per ml of aprotinin, in order to reduce the fibrin degradation.

The experiment was stopped after a total of 5 days and in the fifth day the biological response of the tissues upon external electrical pacing was evaluated. Afterwards, the tissue structure, the organization and the contractile functionality were assessed through histological analysis.



*Scheme 3.1 Schematic experiment strategy for three different replicates: static CRLT, auxotonic stimulation and combination of auxotonic and isotonic stimulation.*



*Scheme 3.2 Flowchart of the experiment strategy for three different replicates: static CRLT, auxotonic stimulation and combination of auxotonic and isotonic stimulation.*

### 3.2.1 Device sterilization

To avoid any contamination and work in an in vitro cell culture environment, a sterilization process is essential. Indeed, the device includes some elements that are in direct contact with the cell environment (e.g. Nitinol posts), and for this reason a sterilization procedure is mandatory.

Since the proof of concept was executed implementing a 3D printed PLA-based prototype, the use of the autoclave instrumentation was not allowed to sterilize it. Consequently, the bioreactor frame, together with the Nitinol posts and the actuation elements (actuator piston and cylinder, tubing and syringe for each implemented bioreactor) were subjected to two sterilization phases:

- a) superficial cleaning using Ethanol solution (70%) for 30 minutes,
- b) exposing to 1-hour UV lights sterilization, under the clean environment of the cell culture hood.

During the second sterilization phase, the components of the bioreactor device were preassembled and then positioned in order to permit the UV lights to reach all the parts and all the elements without the generation of shadows.

Furthermore, the necessary tools to facilitate the sterility practices of the experiment, like the tweezers and the spatulas, were previously sterilized by autoclaving at 121°C for 30 minutes.

### 3.2.2 Neonatal rat cardiomyocytes isolation

The cardiac cells were obtained following an isolation protocol (*N. Tandon, A. Marsano, R. Maidhof, 2007. Neonatal Rat Ventricular Myocytes Preparation Protocol*). After the 0-3-day old neonatal rats sacrifice, the hearts were kept on ice in sterile conditions. Therefore, the rat hearts were

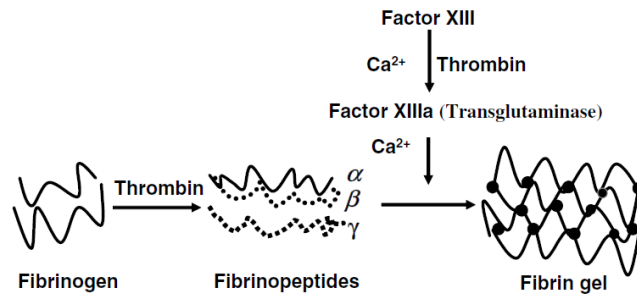
cut in order to remove the atrial part and the aorta. The remaining ventricular tissues were cut themselves to obtain smaller and uniform size pieces. These fragments from the tissue of the ventricles were digested in a trypsin solution overnight, at 4°C agitated at the rate of 50-60 oscillation per minute. For an amount of around 30 hearts, the volume of the trypsin solution was 50 ml (15 mg of the enzyme per 25 mL of Hank's balanced Salt solution *HBSS*).

The digestion was stopped implementing a five-cycle collagenase digestion. Therefore, 10 ml of high glucose Dulbecco Modified Eagle's Medium (DMEM, *Sigma*) supplemented with 1% HEPES (*Life Technologies*), 1% penicillin-streptomycin-fungizone (antibiotic-antimycotic, *Life Technologies*), 1% L-glutamine (*Sigma Aldrich*) and 10% fetal bovine serum (FBS) were added and the sterile collagenase solution was prepared weighing 50 mg of the enzyme per 50 ml HBSS. The five-digestion steps were performed adding 10 ml of collagenase solution at 37°C for 4 minutes with shaking at 170 rpm and collecting the cell suspension. Once the tissue was digested, the cell suspension was centrifuged at 700 rpm for 10 minutes.

After the centrifuge, the cells were resuspended in an appropriate amount of culture medium based on the initial number of the hearts and they were placed in flasks in the incubator for 1 hour, that allows the cells to pre-plate themselves. After 1-hour incubation, , collecting the cell suspension from the flasks and centrifuging (1200 rpm, 5 minutes) it is possible to separate the cardiomyocytes from the other cardiac cells and to determine the cardiomyocytes number using trypan blue solution to exclude dead cells.

### **3.2.3 Fibrin-based cardiac tissues generation**

The reaction of fibrinogen and thrombin lead to the fibrin gel formation (*Scheme 3.3*). The schematic illustration of this reaction is reported by the following figure:



*Scheme 3.3 Schematic illustration of the fibrin gel reaction (Zhao, et al. 2007).*

Beginning from the fibrinogen protein, fibrin gel achievement involves several phases (Zhao, et al. 2008). Indeed, the other fundamental component that allows the fibrin gel formation is the thrombin, with the ability to transform the fibrinogen into fibrinopeptides. Consequently, the action of calcium ions ( $\text{Ca}^{2+}$ ) stimulates Factor XIII to change in transglutamine. The latest promotes the crosslinking between the fibrinopeptides to produce a fibrin network. The stated network represents the structure on which the cells are easily entrapped. The main advantage of the production of fibrin is that the fibrinogen could be obtained autologously, driving to the limitation of virus infection, and in this kind of environment the cells are mostly stimulated to produce collagen and elastin (Zhao, et al. 2007).

Basing on the brief explanation of the process that drives to the formation of the hydrogel, the fibrin construct was generated following four main steps:

- a) cell suspension preparation,
- b) preparation of fibrinogen added with calcium chloride,
- c) mixing of cell suspension and the prepared solution (b) and first positioning of the gel over a silicon mold,
- d) thrombin and aprotinin solution preparation and injection of it on the preexisting fibrinogen-based construct.

In detail, the total amount of hydrogel was 100  $\mu\text{l}$  solution:

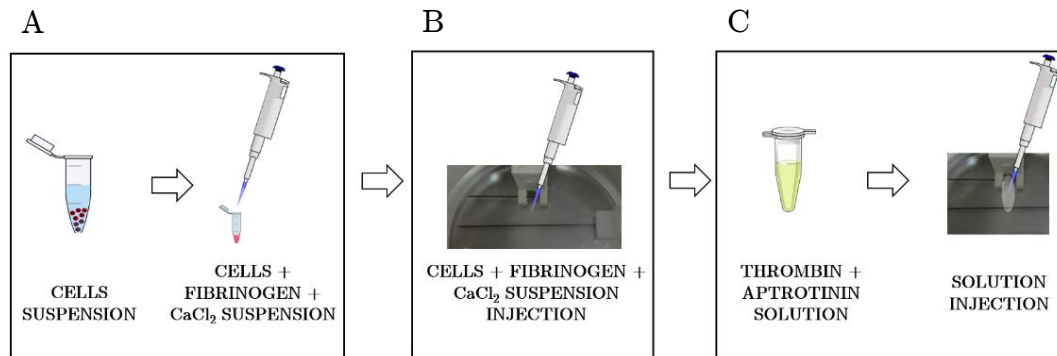
- a) cell suspension (1.8 million cells): 38  $\mu$ l;
- b) fibrinogen (100 mg/ml): 24.8  $\mu$ l;
- c) CaCl<sub>2</sub> (40 mM): 28.9  $\mu$ l;
- d) Thrombin (100 U/ml): 2.5  $\mu$ l;
- e) Aprotinin (40 TIU): 5.75  $\mu$ l;

and the cell were suspended in high glucose Dulbecco Modified Eagle's Medium (DMEM, *Sigma*) supplemented with 1% Hepes (*Life Technologies*), 1% penicillin-streptomycinfungizone (antibioticantimycotic, *Life Technologies*), 1% L-glutamine (*Sigma Aldrich*) and 10% fetal bovine serum (FBS).

Therefore, as summarized by the next scheme (*Scheme 3.4*), the generation of the construct could be described as the succession of the following phases:

- a) cell suspension preparation: 38  $\mu$ l Eppendorf tubes suspension with an amount of 1.8 million cells in each one,
- b) hydrogel formation: addition of the fibrinogen followed by the supplement of CaCl<sub>2</sub> on the cells suspension,
- c) hydrogel positioning: injection of the prepared solution between the two Nitinol rods and over a rectangular shape 3D silicon mold with set size (10 x 4 x 1 mm),

- d) thrombin and aprotinin addition: preparation of thrombin solution added with aprotinin and injection of it on the cardiac construct.



*Scheme 3.4 Schematic representation of the fibrin gel cardiac tissue generation: cell suspension and fibrin gel preparation (A), first part of the gel solution positioning (B) and second amount of solution addition (C).*

The silicon mold was kept in position for an overnight time, in order to assure the polymerization of the fibrin gel, thus the stability of the ECT creation.

### 3.2.4 Biomechanical stimulation of the ECT

As previously mentioned, among the three replicates only two were mechanically stimulated. One ECT construct was subject to auxotonic stimulation and, on the other one isotonic stimulation was applied after three days of culture in auxotonic condition.

To apply both loading condition, the system should not suffer variations and the cardiac tissue should not be moved. Indeed, as the next figures shows (*Figure 3.3*), before starting the sterilization process and then the construct preparation, the actuator piston of the hydraulic system using for the dynamic stimulation was already connected with the clamp linked to the shortest Nitinol rod (*Figure 3.3 (A)*). This advantage was derived by

the solidity of the bioreactor, since all its elements were embedded on the spacer frame, constituting part of the traditional culture dish (*Figure 3.3 (B)*). Therefore, 3 days afterward the construct realization, the cyclic stretching (*Figure 3.3 (C)*) of it was started transferring the syringe to the syringe pump and launching the latter with the planned parameters.

To generate the cyclical stretching motion a 15.5 mm diameter syringes was used. Therefore, using a commercially available syringe pump (Harvard Apparatus PHD 2000) it was necessary to convert flow rate and the delivered volumes in piston velocity and displacement, respectively. Indeed, in order to generate a trapezoidal waveform close to sine waveform (*Graph 3.1*) with displacement stroke equal to 1 mm and 1Hz peak-to-peak frequency, during each cycle, a volume delivery of 226  $\mu\text{L}$  with a slope of 27 mL/min, reproducing the physiological-like condition of 10% strain amplitude and 60 beats-per-minute frequency). The set parameters of the stimulation were kept constant over the 2 days dynamic stimulation.

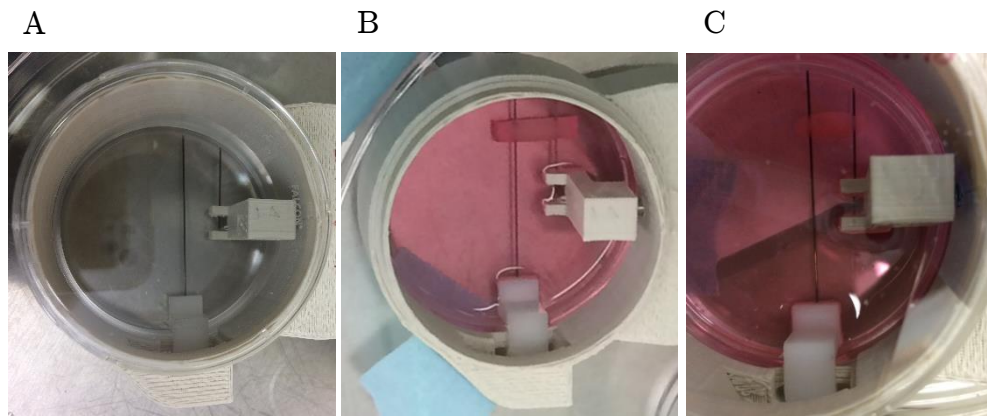
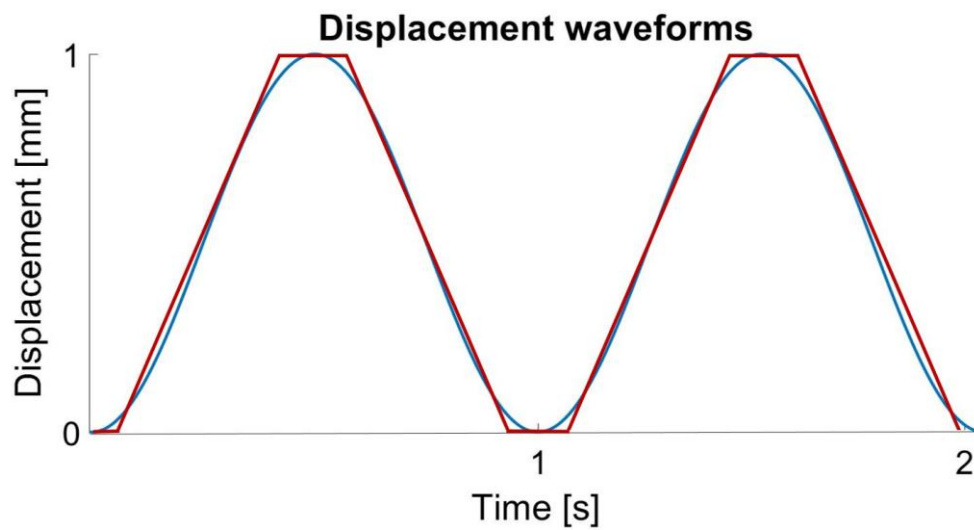


Figure 3.3 Pictures of the assembled bioreactor (A), the dish filled with the culture medium and the ECT positioned over the silicon mold (B), ECT embedded between the Nitinol wires in auxotonic condition (C). The figure C could be represented even for the isotonic stimulation, since the implementation is the same with the additional cyclic transition back and forth of the shortest wire.



Graph 3.1 Example of displacement waveforms imposed using the traditional syringe pump; the sinusoidal waveform (blue color) parameters were reproduced implementing a trapezoidal waveform (red line).

### 3.2.5 ECT characterization

Different functionalizing analysis were implemented after the 5 days experiment in order to characterize the cardiac engineered tissue and to evaluate the biological response due to the combination of auxotonic and isotonic stimulation.

The characterizing tests were based on:

- a) the structure and cell organization analysis through histological evaluation,
- b) the contractility force upon electrical pacing and following measurement of the construct developed force.

#### 3.2.5.1 Histological analysis

After the stop of the experiment running and the electrical simulation tests, the samples were prepared for the histology. Since the in vitro model was generated as a three-dimensional construct, the latest was cut in slices of 10  $\mu\text{m}$  thickness along its longitudinal direction (from the shortest post to the cantilever). The cutting was implemented using a cryostat machine. Indeed, the cutting was preceded by a fixation and then a freezing procedure of the ECTs. The fixation procedure is mandatory to preserve the cellular structure as close as possible to the initial state. This process allows the antigens immobilization, maintaining the cellular and subcellular structure, and it is therefore essential to perform the histological analysis.

#### **Fixing procedure**

The necessary materials to implement the fixing protocol have been:

- a) Phosphate Buffered Saline solution (PBS, 1x diluted),
- b) Paraformaldehyde (PFA, 4% concentrated).

First, the constructs were removed from the bioreactor and placed inside a normal culture dish. They were subjected to two thorough washings with PBS solution in order to remove all the medium residuals. Afterwards, they were covered by PFA solution and they were kept in this condition over night at 4°C.

The day after, the PFA was removed by the dishes containing the ECTs and other two following washing in PBS were carried out to remove the toxicity of the PFA. The described phases allow to obtain fixed construct that could be properly frozen and then cut in thin slices.

### **Freezing procedure**

The fixed samples were frozen using the following protocol:

- a) they were initially embedded in transparent plastic-molds and they were labelled,
- b) each mold, containing half a sample, was filled by OCT solution,
- c) each mold was frozen keeping it inside a backer filled by liquid Nitrogen, thanks to the freezing forceps, until the freezing is complete.

Once the tissues were frozen, they must have been kept at -80°C until use.

### **Cutting procedure**

Once the samples have been properly prepared through the previously described techniques, they were subject to a cutting procedure in order to obtain 10 µm slices thickness, beginning to a three-dimensional sample.

The instrumentation exploited to cut the frozen sample is the Leica Cryostat CM1950. It allows automatic and manual sectioning of the sample. Therefore, for each replicate (static control, auxotonic stimulated and combination of auxotonic and isotonic stimulated one), they have been cut using the manual procedure. Afterwards, the 10  $\mu\text{m}$  cuts thickness were mounted in several histology slides.



---

*Figure 3.4 Picture of the exploited CM1950 tool of the Histology Core Facility of the Department of Biomedicine (Basel, Switzerland).*

#### **3.2.5.1.1 Immunoistochemical evaluation**

The immunoistochemical tests were implemented exploiting the continuous linear automatic stainer (COT 20) for the hematoxylin and eosin staining (H&E), that represents one of the principal stainings in histology.



*Figure 3.5 Picture of the exploited COT 20 tool of the Histology Core Facility of the Department of Biomedicine (Basel).*

The mentioned instrumentation is easily usable to obtain an immunohistochemical analysis, since the protocol is carried out almost automatically by the COT 20. The implemented protocol makes use of Papanicolaou's solution 1a Harris' hematoxylin solution and a mixture of Eosin and Erythrosin B. The phases of the procedure are a cyclical set of exposures of the tissue slides to different solvents and solutions, including HE Papanicolaou solution and Eosin 1% supplemented by Erythrosin B 1%. Therefore, the stain protocol for COT 20 could be explained by the following table:

*Table 3.1 Phases of the H&E protocol.*

<b>Time (seconds)</b>	<b>Steps</b>
120	XTRA-SOLV
120	XTRA-SOLV
120	XTRA-SOLV
120	EtOH 100%

120	EtOH 100%
120	EtOH 70%
120	EtOH 50%
120	H <sub>2</sub> O distilled
120	HE Papanicolaou J. T. Backer: 3873
120	H <sub>2</sub> O tap
120	HCl Alcool 0.2%
120	H <sub>2</sub> O tap
120	H <sub>2</sub> O tap + NH <sub>4</sub>
120	H <sub>2</sub> O distilled
120	H <sub>2</sub> O distilled
120	Eosin 1% + Erythrosin B 1%
120	Eosin 1% + Erythrosin B 1%
120	H <sub>2</sub> O tap
120	EtOH 96%
120	EtOH 100%
120	XTRA-SOLV
120	XTRA-SOLV

As the table shows, after 52 minutes the slides, thus the tissues, have been subject to different solutions. Tissues stained by this method show:

- a) nuclei in blue/purple,
- b) cytoplasm in red,
- c) mitochondria in pale pink.

### 3.2.5.1.1 Immunofluorescence evaluation

Immunofluorescence is an essential technique used to determine the location of antibodies or antigens in tissues in which the antibodies or antigens of the existing structures are labelled with a fluorescent dye (*Collins English Dictionary, HarperCollins Publishers*).

The histology tissue slides prepared with the cutting tool have been submitted to a fluorescence staining protocol. To implement it, the necessary materials and solutions have been:

- a) PBS,
- b) Staining buffer: 0.3% Triton X-100 and 2% normal goat serum in PBS or if primary antibody was produced in goat, serum or 0.5% BSA,
- c) primary and secondary antibodies solutions.

The first stage has been the PBS wash of the tissue for at least 10 minutes. Afterwards, the PBS must be removed and the slides must be positioned in humid chamber. Therefore, the staining buffer has been left for 1 hour (ca. 100  $\mu$ l per section).

To prepare the primary solutions, either goat polyclonal anti-vimentin or mouse monoclonal IgG1 anti-sarcomeric  $\alpha$ -actin was added as primary antibodies to the blocking solution with 1:100 dilution. Anti-sarcomeric is specific for the  $\alpha$ -cardiac actinin. Once the primary solution was injected on the tissue sections, they were incubated in the dark in fluorescently labelled anti-rabbit and anti-goat secondary antibodies (1:200).

Furthermore, cells nuclei were stained using DAPI (Invitrogen) at 1:150 dilution for 1 hour. Antibodies were diluted in 0.3% Triton X-100 and 2% normal goat serum in PBS.

The final steps of the protocol regard the mounting of the histology glasses with mounting medium and the storing of them at 4°C after drying.

To analyse the fluorescent staining results, images were taken with the microscope. Indeed, fluorescent contrast has been essential to detect on the images the blue colour of the DAPI and the green one of the  $\alpha$ -sarcomeric actin.

### 3.2.5.2 Electrical pacing

Regarding the external electrical stimulation of the replicates, it was implemented exploiting the principle of functioning of electrical circuit described in the *section 2.2.3* of the document.

Moreover, the live imaging microscope Olympus ZEISS X81 was used to electrically stimulate the cardiac tissue. Indeed, it offers a cell culture environment, because it is equipped with an incubator on which 37°C temperature and 70% humidity are preserved. Therefore, the external pacing was performed positioning the microscope-based bioreactor with the ECT on the optical system.

The Nitinol posts, used as electrodes, were connected through electrical terminals to the stimulator and then it was actuated.

The electrical pulses were imposed to the cardiac tissue increasing the voltage value, beginning from 1 V, in order to measure the minimum electrical field able to generate a beating tissue following the pacing (Excitation Threshold, ET). Once from the live imaging was shown a synchronous beating of the tissue in response to the stimulation, the voltage value was considered as ET. Therefore, keeping constant the amplitude the frequency values was gradually changed (from 1 Hz up to a maximum of 10 Hz) in order to estimate the maximum capture rate (MCR) of the testing ECT. The maximum capture rate represents the maximum imposed frequency that the tissue can follow during the pacing.

### 3.2.5.3 Force measurement test

The recording of the electrical pacing tests has allowed to obtain videos of the beating constructs. These videos were properly elaborated through a Matlab code in order to quantify the cantilever deflection, consequently to calculate the active force of the ECT during the contraction.

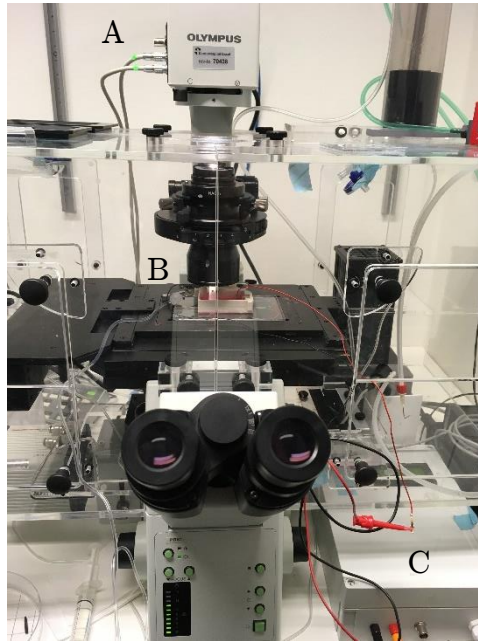


*Figure 3.6 Picture of the electrical pacing test setup: live imaging microscope (A), bioreactor positioning in the middle (B) and electrical stimulator on the right bottom (C).*

The videos were acquired with 86 frames per second and they were then compressed. Only a representative section of the video was considered and used to quantify the cantilever deflection on Matlab. Indeed, the video was conceived as a series of frame and for the force measurement the segmentation principle of functioning implemented for the characterization of the isotonic stimulation module was exploited. Therefore, detecting the changing of the centre of mass of the tissue portion considered (thus the cantilever displacement due to the contractile force developed), the trend of the cantilever displacement was calculated. The latest has then allowed to obtain the average force measurement.

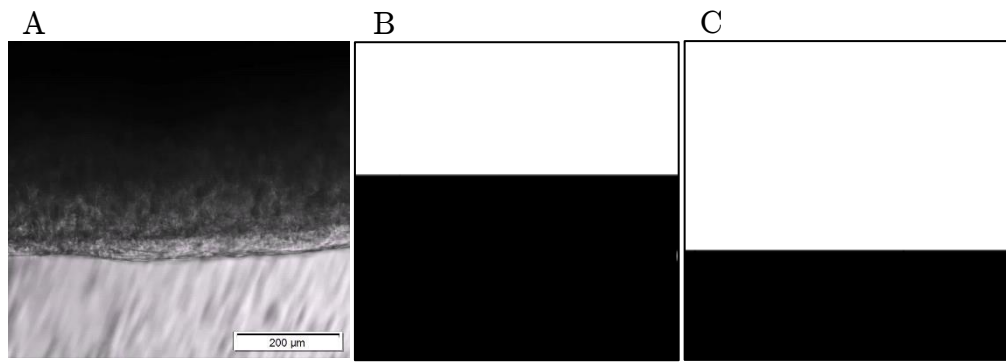


*Figure 3.7 Representation of the main steps of the ECT force quantification: photomicrograph of the recorded video during the pacing (A) on which the darkest part represents the tissue casted on the cantilever; examples of segmented frame of the video where the with rectangular shape represented the contraction area of the tissue during the beating: position 1 (B) and position 2 (C).*

## 3.3 RESULTS

### 3.3.1 Histological results

The immunoistochemical results (*Figure 3.7*) have shown that there are important differences in the structure of the three replicates. In static condition the cardiomyocytes have organized themselves in multidirectional structures and mainly around the fibrin gel edges. Furthermore, in the images acquired from the ECT subjected to the auxotonic stimulation conditions for 5 days it was possible to evaluate that the cells were structured mainly along the direction of the imposed load. This effect has been even more found in the images regarding the cardiac tissue exposed to the combination of auxotonic and isotonic stimulation.

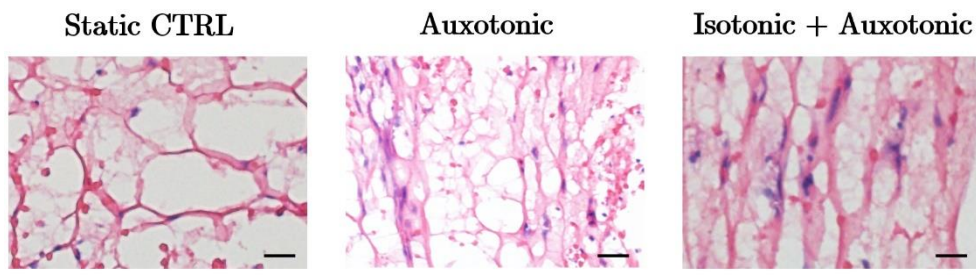


*Figure 3.8 Example of histological images for the three conditions. The nuclei are visualized in blue, while the pink color represent the structural component (scale bar 50  $\mu$ m).*

The previous results were confirmed by the immunofluorescence staining (*Figure 3.8*). The results have shown the presence of the  $\alpha$ -sarcomeric actin. This result confirms that the structures observed in the H&E stainings are formed by cardiomyocyte myotubules.

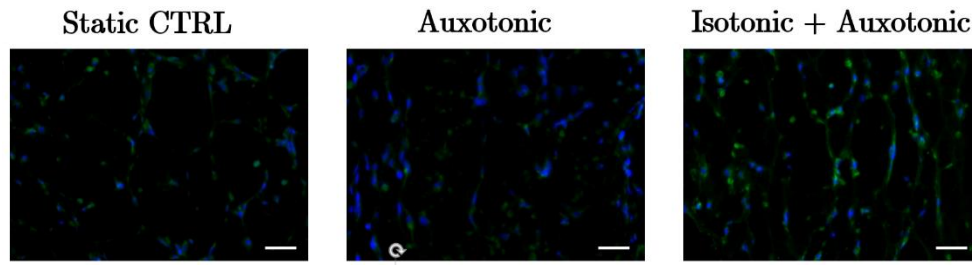
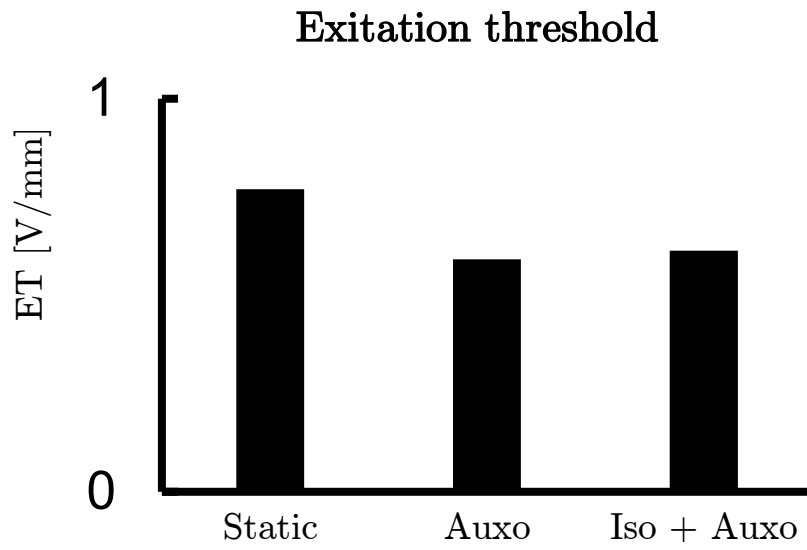


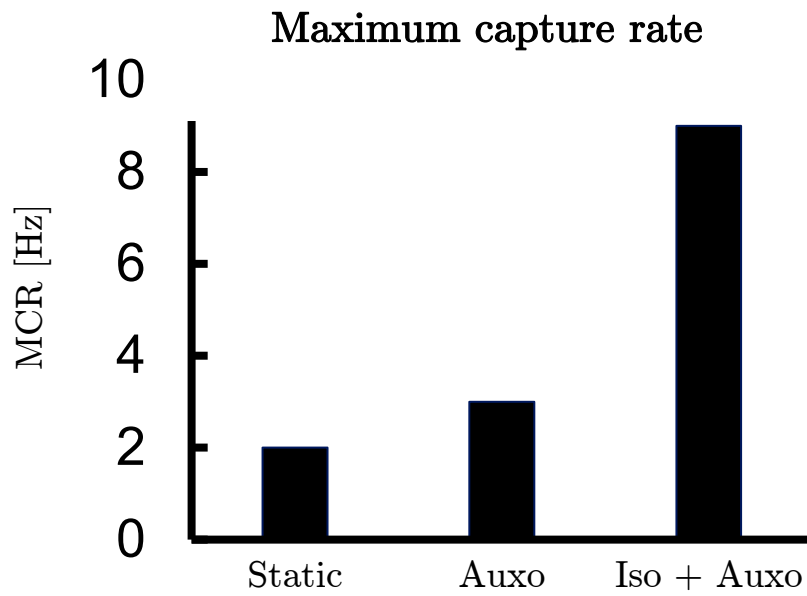
Figure 3.8 Example of fluorescence images for the three conditions. The nuclei are visualized in blue (DAPI), while the green color represent the presence of  $\alpha$ -sarcomeric actin (scale bar 50  $\mu\text{m}$ ).

### 3.3.2 Electrical pacing result

The presence of matured cardiac structure was also confirmed by the results obtained by the electrical pacing. The electrical test allowed to know the excitation threshold value and the maximum capture rate for each replicate. The ET represents the minimum electrical field able to generate a beating tissue following the pacing and it was calculate dividing the minimum registered voltage value for the distance between the electrodes (10 mm). The results have shown that ET is lower in the replicates on which auxotonic and both auxotonic and isotonic stimulation were applied (*Graph 3.2*). Moreover, MCR is higher the ECT that was subjected to the isotonic mechanical stimulation (*Graph 3.3*).



*Graph 3.2 Excitation threshold values for the three conditions.*

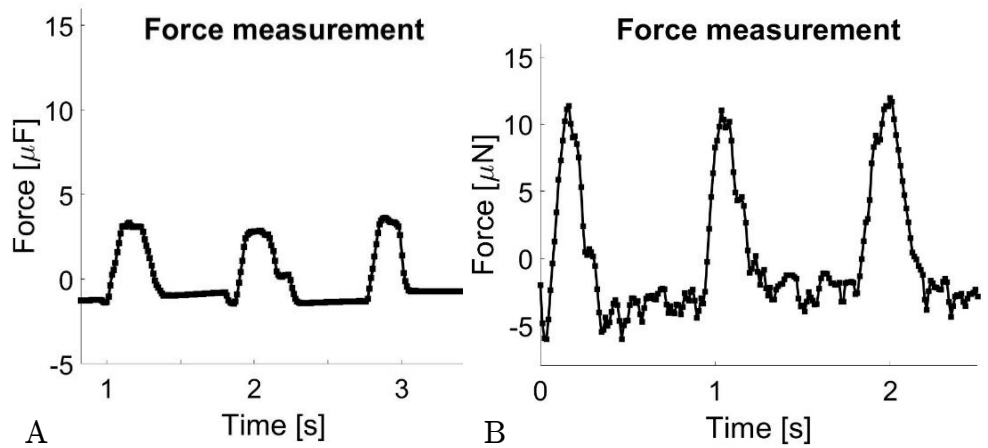


*Graph 3.3 maximum capture rate values for the three conditions.*

These results suggested that the physical loading of the cardiac tissue promote the electrical properties development, since these replicates have been able to follow the external stimulation without the need to reach high value of voltage and they have revealed the capability to follow it for higher frequency values.

### 3.3.3 Force measurement results

As previously mentioned, the live imaging microscope has been advantageous to evaluate the contractile force due to the electrical pacing, since the contraction produced a displacement of the cantilever. The acquired video of the electrical stimulation was elaborated implementing a Matlab routine and the cantilever calibration was also used (*section 2.2.1.1*).



*Graph 3.4 Examples of plots of force measurements during the external electrical pacing test: ECT subjects to auxotonic condition (A) and ECT on with the combination of auxotonic and isotonic stimulation was applied (B).*

The graphs showed that the developed force was higher on the tissue that was submitted to two stimulation conditions (averaged force value: 15 micro Newtons) than that one measured during the test of the ECT stimulated in auxotonic condition (average force value: 4.42 micro Newtons)

### 3.4 DISCUSSION AND CONCLUSIONS

It is well-known that biomimetic approach plays an essential role on generation of functional engineered cardiac tissue models. Mechanical stimulation produces beneficial effects on myocardial tissue development stage and in its performance, because it aims to reproduce the heart preloaded and afterloaded conditions of the contraction cycle (*Zimmermann, et al. 2013*). To apply biophysical stimuli to ECTs, implementation of suitable instrumentation is fundamental. Bioreactors could create the ideal environment to generate and to characterize an engineered tissue. For this reason, available numbers of bioreactor devices have been developed in the last decades.

Since several tests would be necessary to thoroughly study the effects of the stimulation and the construct's properties, the strong need to obtain a bioreactor able to provide results with as less as possible materials motivates research studies. In this context, Kensah's group has developed a bioreactor in order to test miniaturized bioartificial heart tissues, enabling small-scale cardiac tissue investigation (*Kensah, et al. 2011*). The latest was able to apply cyclic strain to myocardial tissues, thus dynamic stimulation, to evaluate the effects of it compared to the static control replicate, as others comparable devices developed in CTE research groups (*Zimmermann, et al 2002. Birla, et al. 2007*). However, different types of mechanical stimulation can be applied. Together with static and dynamic loading (respectively related to isometric and isotonic contraction), the quasi-static condition (auxotonic loading) should be considered in the analysis of the ECT models. Indeed, it represents a combination of isometric and isotonic contraction and it was demonstrated that passive preload is essential to train the tissue and to improve maturation process, but there is no device able to provide both quasi-static and dynamic loading with the same implementation and the same instrumentation involved.

Moreover, electric stimulation positively influences the heart tissue functionalization. It seems to induce a similar degree of cardiac myocyte

differentiation as mechanical stimulation (*Vunjak-Novakovic, et al. 2010*). To implement it, bioreactors can be equipped with electrodes in order to apply electric stimulation. For example, in Birla's manuscript, a method to transfer electrical stimuli on ECTs was presented (*Birla, et al. 2007*). In the mentioned research study, electrical stimulation was applied using parallel platinum electrodes, and the active force was measured using an additional force transducer.

Furthermore, although it is recognized that a real-time monitoring is advantageous to conduct a depth investigation of the model development and testing, the existing tools used in cardiac tissue engineering have architectures that make hard to perform microscopy analysis. Devices directly usable with traditional microscopy systems facilitate to capture microscale observation of the ongoing experiment.

Characterization and optimization of a novel microscope-based bioreactor for mechanical training of cardiac engineered tissues was the main aim of this master thesis project. It was designed in order to be integrable in microscopy systems through traditional cell culture tools and it was able to provide both macroscale and microscale observation during the functioning. Moreover, the bioreactor was conceived to be miniaturized in order to guarantee the generation and then the functionalization of a meso-scale tissue. This concept has been advantageous in terms of costs, since a material reduction was possible, but even meso-scale tissue has represented a great balance between macro and micro-scale constructs. Indeed, a meso-size could offer both tissue functionality results and molecular investigation. Firstly, optimization of the bioreactor modules has driven to gain the delivering of physical stimuli on cardiac tissue. Consequently, the bioreactor was capable to implement different conditions of stimulation (auxotonic and isotonic) and to change the pattern of stimulation, enabling either mimicking of native or pathologic environments.

The validation of the device as a proof of concept was conceived to quantify the feasibility of it in the biological context. The cardiac tissue was 3D fibrin-based produced, it was suspended between two holders, that

allowed to apply mechanical and electric stimulation. The choice behind the fibrin use as a material to embed the cardiomyocytes was driven by fibrin' s own properties. Indeed, the primary constituent of the fibrin (fibrinogen and thrombin) can be isolated from blood samples and the polymerization process is easily implementable. Furthermore, the degradation of fibrin gel can be controlled by protease inhibitors (e.g. aprotinin) and such a polymer is known to stimulate the secretion extracellular matrix proteins by seeded cells (*Jockenhoevel and Flanagan, 2014*).

Consequently, the engineered tissue functionalization was performed to evaluate the biological response.

The proof of concept experiment has allowed to attest the ease of implementation of the device and the efficient sterility maintenance during its functioning. Moreover, the validation has demonstrated the capability to guarantee the cells environment and maturation, as well as the preservation of the initial imposed conditions.

Dynamic and quasi-static stimulations were performed providing the loading conditions pre-characterized on the calibration phases. Auxotonic stimulation has promoted the self-organization of the cardiac cells inside the fibrin matrix, enabling the development of a passive force that could be quantified thanks to the force sensor. Isotonic stimulation was applied on the construct after 3 days of pre-loading condition, avoiding submitting the construct to cyclic strain without a proper previous training of it. The dynamic loading has applied 10% stretch on the tissue length (1 millimetre over total 10 millimetres length), cyclically at the frequency of 1 hertz.

Electric stimulation was imposed on the tissue after 5-days experiment in order to evaluate the contractile force developed from it. The excitation test of the tissue has revealed that auxotonic and isotonic stimulation have developed positive feedback regarding electric properties of the tissue. Indeed, as well as mechanical stimulation is essential to mimic the mechanical milieu of the heart tissue, it is also beneficial to explain electric functionality of the tissue. Therefore, biomechanical stimuli have

driven to a well-defined cell alignment along the loading direction and the alignment has allowed to obtain more efficient electric connections on the tissue environment. That was highlighted firstly from the histology results and secondly from the electric parameters and active force measurements.

H&E results were fundamental to observe cardiomyocytes organization. While the static control ECT was defined by a multidirectional orientation structure, on which the cells were organized around the fibrin matrix edges, the mechanically loaded ECTs have shown an ordinate architecture, on which the nuclei were aligned enabling myotubes formation. Furthermore, results obtained from the alfa-sarcomeric actin staining were assured that the engineered tissue was mainly structured by cardiomyocytes, with mechanical and electrical properties. This was also confirmed by the excitation threshold values measured during the external pacing: combination of quasi-static and dynamic contraction has promoted the efficiency of response to electric field exposure. The response success was even shown changing the frequency of the electric stimulation on the tissue. The loaded cardiac construct could follow synchronically the pacing at higher frequency values than the ones measured on the control one. Moreover, active force measured during the electric pacing was markedly different in the stimulated ECTs. The tissue on which combination of auxotonic and isotonic stimulation was applied has developed an average force value that is almost three times greater than the one measured on the ECT that was submitted to 5-days quasi-static contraction.

## 4 CONCLUSIONS AND FUTURE PROSPECTIVE

---

### 4.1 MINIATURIZED MICROSCOPE-BASED BIOREACTOR FOR MECHANICAL TRAINING OF ENGINEERED CARDIAC TISSUE

In this master thesis the characterization of a miniaturized microscope-based bioreactor for mechanical training of ECT has been presented. It was conceived to be characterized by a miniaturized and modular architecture to allow mesoscale cardiac tissue culturing and training and in order to guarantee the ease of microscopy monitoring and analysis.

The main idea behind the device application was the low-cost development. The modularity of the bioreactor frame has driven to the advantages to gain basic design and simple manufacturing. The modules of functioning of the device were implemented without the need to include additional instrumentations or sensors: the force measurement could be implemented easily with the cantilever use and the displacement analysis during the cyclic stretching of the tissue was implemented through the microscope. Moreover, characterization of these modules is valid in different size and design version of the frame, meaning that the functioning modules could be easily adapted and implemented in different design versions.

However, this device has presented other significant and innovative strategies. It was conceived to culture cardiac tissues and to cast it, enabling a biomimetic approach implementation. Indeed, the tissue was embedded between two metal posts made in Nitinol. The Nitinol wires as rods to cast the tissue constitute a great innovation in this context, since both Nitinol mechanical and electrical properties have been advantageous on the bioreactor implementation. They have permitted to combine quasi-static and dynamic contraction on the cardiac tissue, as well as the electrical parameters evaluation. Regarding the mechanical stimulation several concepts of its implementation were inventive. Taking advantage of the use of hydraulic system to deliver the mechanical stretching on the constructs,

rigid connection and vibration on the system were prevented. Moreover, the stimulation was delivered using traditional tools of cell culture environment as syringe pumps, enabling even in this way the low-cost development and the easily implementation. The displacement-controlled strategy behind the cyclic loading of the tissues has represented another novel approach. That technique has been advantageous to generate generical displacement waveforms both exploiting an already existing algorithm programmed on the motor stepper software and using the syringe pump programs. Furthermore, displacement-controlled strategy has driven to execute a stability check of the system just using a microscope objective as displacement sensor and to develop an easier analysis of the errors of the mechanical stimulation system (e.g. drift error).

On the other hand, ECTs electric stimulation has been performed exploiting the Nitinol wires. Since the heart tissue was casted between the metal posts, they could be used to apply an electric field to the heads of the tissue: there was no need to connect the construct to suitable electrodes. Here again this approach has led to the full use of the properties of the elements constituting the device, that was the main aim of the designed bioreactor.

Not only the complete utilization of the bioreactor components has been advantageous to reach a low-cost development of the first prototype. Indeed, beginning to the Solidworks 3D drawings (reported in appendix), the bioreactor frame prototype was realized using 3D printers. They have assured the obtention of good quality products with high precision and speed together with low-cost prototyping.

## **4.2 PROOF OF CONCEPT**

The biological validation of the first prototype was implemented to evaluate the bioreactor functionality and stability in the biological environment. Certainly, the sterility maintenance together with the culture

condition preservation have represented the main issue of the the feasibility study. Moreover, the biological test was executed in order to validate the fibrin gel functionality and stability as matrix on which the cells must be able to create a heart tissue. The exploitation of that hydrogel as construct has reported efficient results and the formation of such a material on which the cardiomyocytes were embedded has been easy to develop.

The proof of concept has shown the possibility to obtain reliable mechanical stimulation on cardiac tissues, enabling to acquire differences in tissue structure and properties compared to the static control. Regarding the dynamic mechanical stimulation, cyclic stretch was produced mimicking the native heart mechanical conditions, without undermining tissue maturation, giving the possibility to apply different patterns of stimulation (e.g. pattern simulating heart pathologies).

The functional tests were conducted after the experiment in order to evaluate the biological response of the tissue. Both histology and pacing evaluation were performed without difficulty. They have shown that the first proof of concept has been successful, beginning to the hypothesis behind the running of the experiment. Indeed, concerning that, the results have shown that combination of auxotonic and isotonic stimulation seem to improve the maturation of the engineered cardiac tissues.

### **4.3 LIMITATIONS**

The first prototype could be optimized to improve the functionality of the device. Firstly, although three-dimensional printers have represented really an advantage on the prototype, different materials and manufacturing techniques could be implemented in order to obtain:

- a) repeatable architecture,
- b) higher precision,
- c) autoclave usability.

Furthermore, flexibility of the longest wire used for the auxotonic implementation could create a deflection during the dynamic mechanical stimulation. Indeed, the tissue is grappled on the two wires and the cyclic translation of the steady short one produces isotonic stretching on the tissue but even it drags the flexible longest back and forth. That has not represented a great issue, since the deflection produced was negligible and insignificant compared to the strain applied on the tissue (10% of the total length). Moreover, the deflection of the longest Nitinol post could be either easily quantified through a real-time microscope monitoring or a fixed pin could be positioned in order to avoid the rod deflection during the cyclic loading.

Since only one experiment has been run, only one experiment time plan was implemented. A longer exposition to auxotonic and isotonic stimulation, or even different timeline combination could be studied to find the most efficient condition to obtain a physiological-like cardiac tissue. Indeed, similar experiments regarding mechanical stimulation of NRCM-based engineered tissues were ran for 10 days (*Hansen, et al. 2010*). As well as, different patterns of stimulation, changing the strain percentage of the tissue and the frequency could be motivated to drive innovative studies regarding heart injuries and drug discovery for novel treatments.

Concerning the external electrical pacing test, it could be applied during the experiment. In that way, electrical parameters and contractility active force development could be evaluated in different phases of the tissue maturation. In the described biological validation, the electrical stimulation of the bioreactor was applied only once that the experiment was stopped (after 5-days experiment). Indeed, one of the limitation of the use of 0.4 mm diameter Nitinol wires is their ease of passivation under electrical pulse in a long-duration applications. For this reason, electrical pacing could be executed during the experiment running and in the long time applying a material reinforce (e.g. PDMS, silicon) on the contact point on which the electric terminals will be connected.

## 4.4 FUTURE WORKS

To make practical the bioreactor usability, front-end software could be implemented in order to be part of the device instrumentation. Certainly, such a software could be running on electronic tools typically used (e.g. laptop, tablet). That would represent a great gain on the user point of view, meaning that everyone could be the user, without the knowledge regarding the technical principles behind the main device functionalities. Therefore, the user could easily set the actuation of the ECTs mechanical stimulation, to change the main parameters of it or stop it thanks to a suitable front-end software implemented on an electrical tool. Moreover, the software would include image processing routines that were implemented on Matlab during the characterization phases of the bioreactor. Indeed, since the bioreactor can be integrated in microscopy instrumentation, these routines on the software could be used to screen and to evaluate the tissue maturation and the contractile force development and to easily monitor the mechanical stimulation parameters through the image processing approach. Then segmentation of the video acquired during the stimulation or segmentation enabling to evaluate the cantilever deflection in auxotonic condition or during electrical pacing could be easily gained.

As further step on the bioreactor validation, the exploitation of other cell lines could be fundamental. The engineered cardiac tissue could be generated using human cardiac cell derived, like for example using human derived iPSCs (Induced pluripotent stem cells). That would be advantageous to drive studies regarding stem cells differentiation and then tissue development and effects of tissue mechanical training. Moreover, using already human iPSCs, biological tests could be executed mimicking in a better mode the human condition.

On the other hand, next biological experiment could demand a higher number of replicates, in order to acquire statistical results of different test combinations. In the view of this purpose, the bioreactor design could be easily adapted to multi-wells culture plates (6, 12, 24 replicates in one dish), without the need to implement a new characterization of the device.

Moreover, either in vitro creation or training of other types of human tissue could be a great achievement. Striated muscle tissue or cartilaginous tissue could be generated and trained on the bioreactor presented in this thesis. Indeed, several tissues constituting the human body show beneficial effects due to mechanical or electrical stimulation. Using different tissues, the principle of functioning and the main modules of the device would not change, but and the functioning parameters could be adapted to different physiological-like stimulations. Like that, the bioreactor would represent a general device usable in several tissue engineering fields.

## 5 ACKNOWLEDGEMENTS

---

Ringrazio innanzitutto il Professor Umberto Morbiducci per avermi dato la possibilità di svolgere questo progetto di tesi all'estero, per i suoi insegnamenti e per avermi seguito costantemente durante tutto il percorso. Allo stesso modo, desidero esprimere la mia più sincera gratitudine ad Anna Marsano, per avermi calorosamente accolta nel suo gruppo di ricerca, per i preziosi consigli e per avermi supportato in ogni fase del lavoro con straordinaria professionalità. Un ringraziamento speciale va, inoltre, a Giuseppe Isu, per la sua dedizione e simpatia, per essere stato un tutor ma anche un amico nei mesi di tesi a Basilea, che quotidianamente mi ha indirizzato nel lavoro, insegnandomi tanto, incoraggiandomi a superare le prime difficoltà e credendo sempre in me.

Ringrazio anche tutto il gruppo di ricerca del quale ho fatto parte, e il Dipartimento di Biomedicina dell'Università di Basilea. In particolare, Diana e Laia per avermi pazientemente introdotto nel mondo della cultura cellulare e per avermi sempre aiutata e sostenuta, insieme a Vladislav, Francesca e Deborah per i momenti condivisi in laboratorio. Ringrazio tutte le persone speciali che ho avuto il piacere di conoscere. I miei compagni di viaggio, Davide, Federica, Chiara, Emma, Francesca, Deborah, Lele, Mattia, con i quali ho condiviso i momenti più significativi di questa bella avventura, e Sébastien per i consigli e il sostegno speciale nell'ultimo intenso mese di lavoro.

*Last but not least*, vorrei ringraziare i miei genitori per aver sempre creduto in me e per avermi incoraggiata in questa esperienza, per essermi stati vicino durante i mesi all'estero, ma anche durante tutti gli anni di studio, perché con l'affetto e il sostegno che mi hanno dimostrato rendono questo traguardo prezioso. Allo stesso modo, ringrazio mia sorella Fabiana e i miei più cari amici, che per me rappresentano sempre un bellissimo e speciale punto fermo. Ringrazio infine i miei colleghi di studio, vecchi e nuovi, e le mie

coinquiline Claudia, Silvia e Luna per aver condiviso con me la vita studentesca a Torino.

## 6 APPENDIX

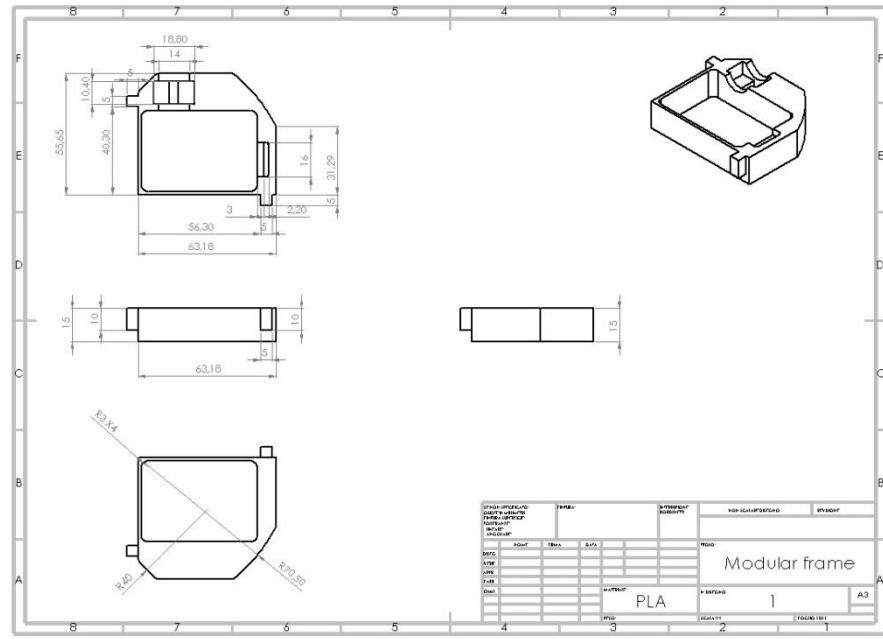


Figure 6.1 Mono-chamber frame drawing.

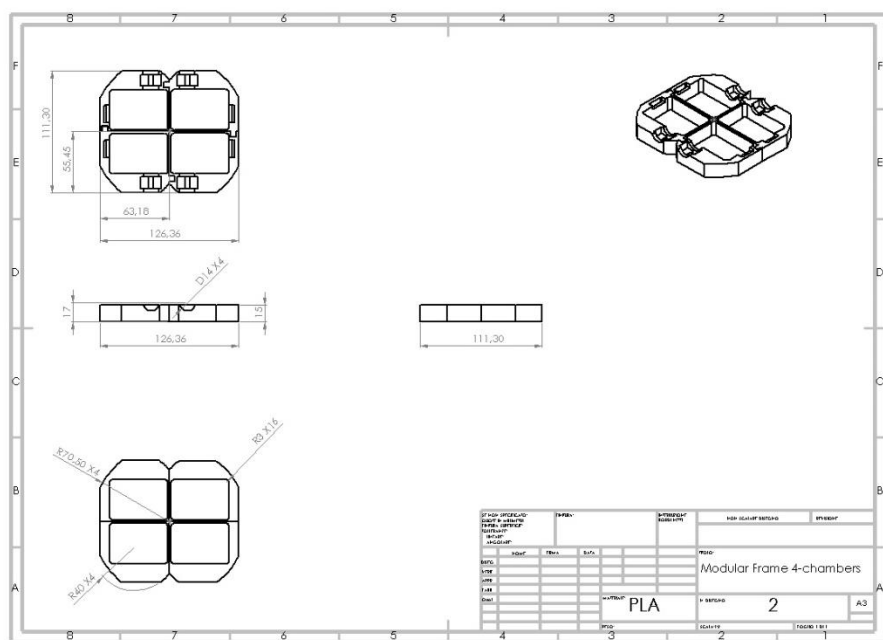


Figure 6.2 Four-chamber modular frame drawing.

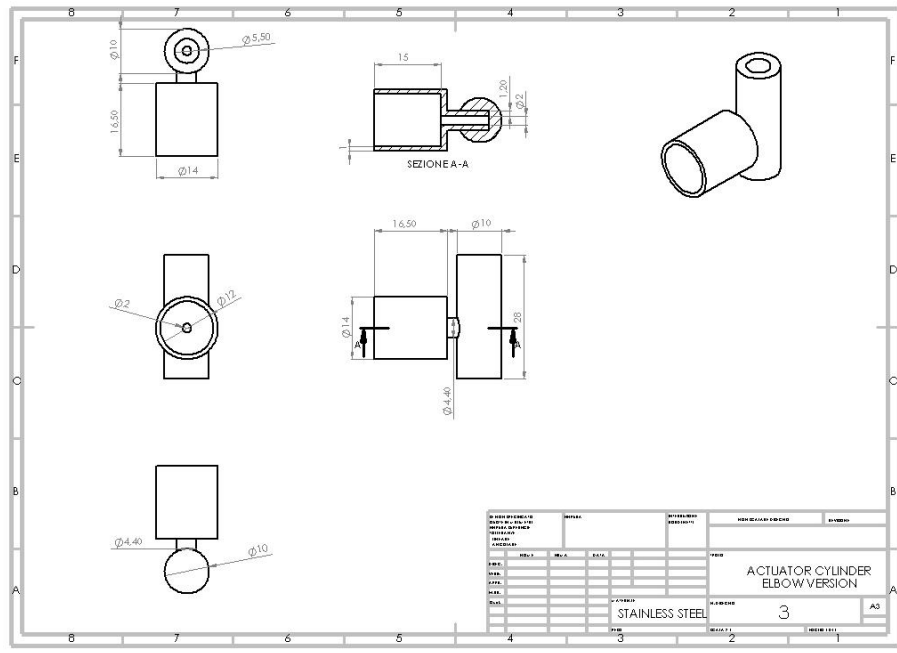


Figure 6.3 Actuator cylinder drawing: elbow version.

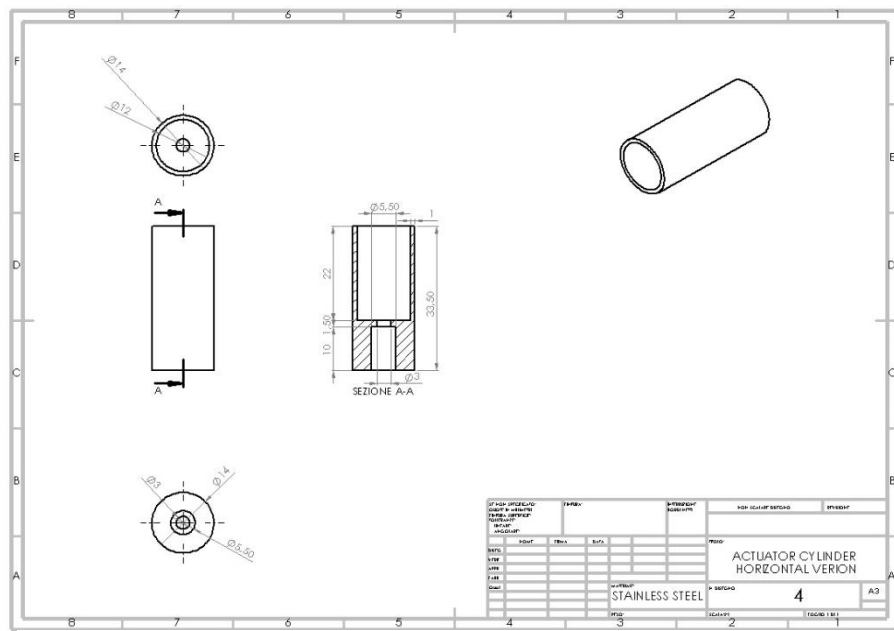


Figure 6.4 Actuator cylinder drawing: horizontal version.

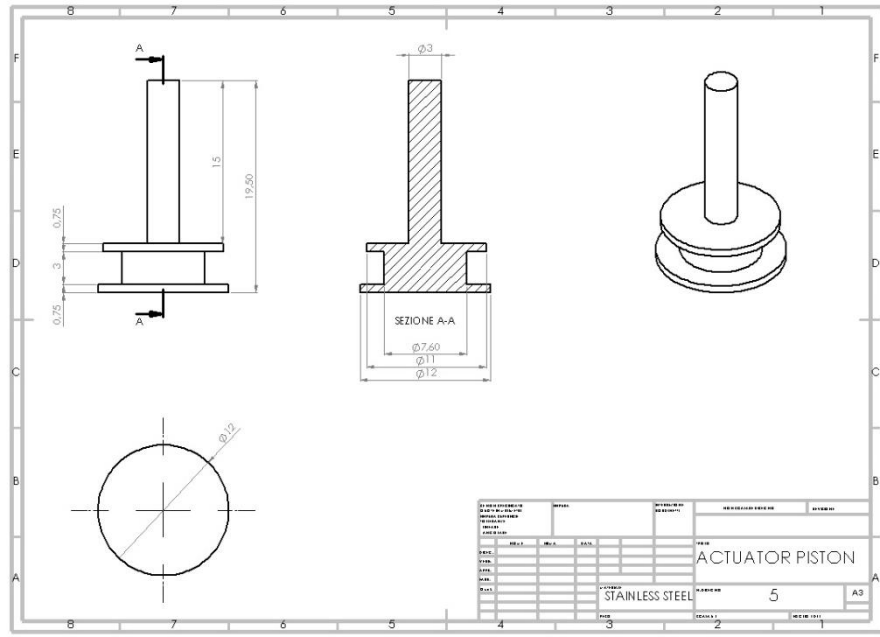


Figure 6.5 Actuator piston drawing.

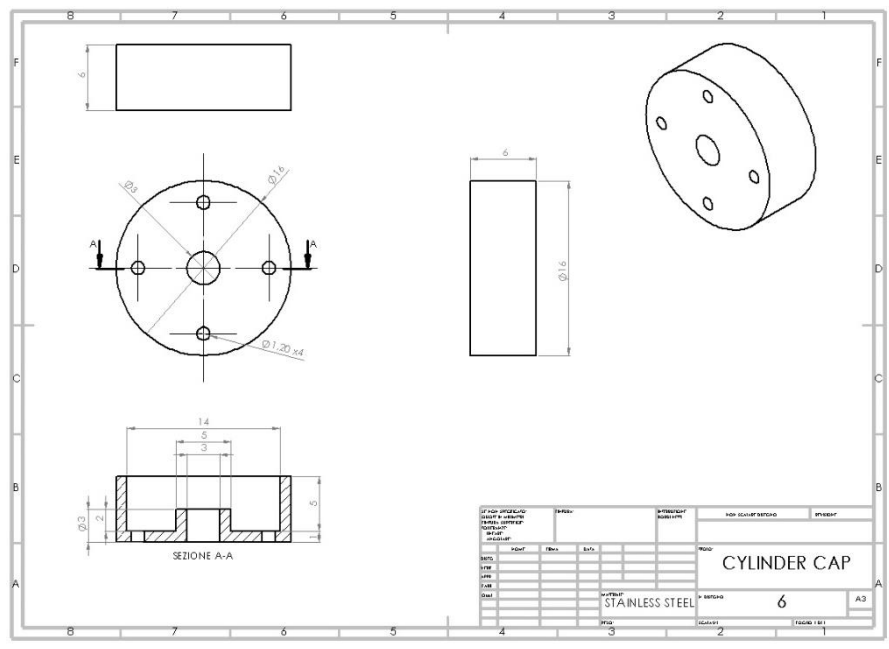


Figure 6.6 Actuator cylinder cap drawing.

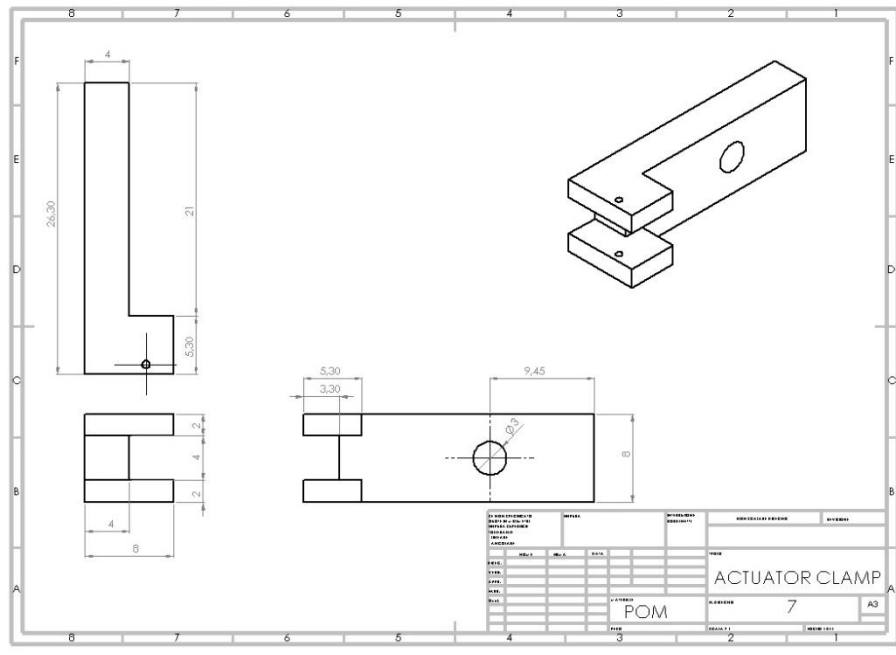


Figure 6.7 Actuator clamp drawing.

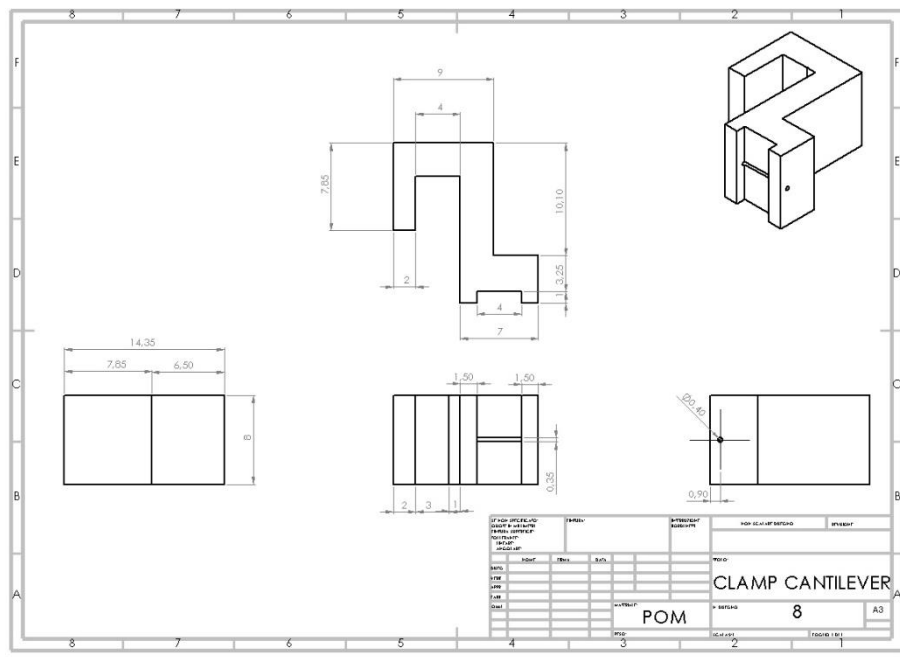


Figure 6.8 Cantilever clamp drawing.



## 7 BIBLIOGRAPHY

---

Roger VL, Go AS, Lloyd-Jones DM, Benjamin EJ, Berry JD, Borden WB, Bravata DM, Dai S, Ford ES et al. "Heart disease and stroke statistics - 2012 update: a report from the American Heart Association". *Circulation*, 2012 ;125(1): e2-e220.

D. Massai, G. Cerino, D. Gallo, F. Pennella, M. A. Deriu, A. Rodriguez, F. M. Montevicchi, C. Bignardi, A. Audenino, and U. Morbiducci. "Bioreactors as Engineering Support to Treat Cardiac Muscle and Vascular Disease". *Journal of Healthcare Engineering*. Vol. 4, No. 3, 2013 – pp.329-370.

Thomas Eschenhagen and Wolfram H. Zimmermann. "Engineering Myocardial Tissue". *Circulation Research*, 2005. 97:1220-1231.

Wolfram H. Zimmermann. "Biomechanical regulation of in vitro cardiogenesis for tissue-engineered heart repair". *Stem Cell Research & Therapy*, 2013, 4-137.

Herman H. Vandenburg, Patricia Karlisch, and Lynne Farr. "Maintenance of highly contractile tissue-cultured avian skeletal myotubes in collagen gel". *In Vitro Cellular & Developmental Biology*, 1988, Vol. 24, No. 3, Part I.

L. Terracio, L. Rönstrand, A. Tingström, K. Rubin, L. Claesson-Welsh, K. Funai, and C. H. Heldin. "Induction of Platelet-derived Growth Factor Receptor Expression in Smooth Muscle Cells and Fibroblasts Upon Tissue Culturing". *The Journal of Cell Biology*, 1988, Vol. 107, 1947-1957.

W. L. Stoppel, D. Hu, I. J. Domian, D. L. Kaplan, and D. Black III. "Anisotropic silk biomaterials containing cardiac extracellular matrix for cardiac tissue engineering". *Biomed. Mater.*, 10, 2015, 034105.

Valerie F. Shimko, and William C. Claycomb. "Effect of Mechanical Loading on Three-Dimensional Cultures of Embryonic Stem Cell-Derived Cardiomyocytes". *Tissue Engineering*, Part A, Vol. 14, No. 1, 2008.

N. Y. Liaw, W. H. Zimmermann. "Mechanical stimulation in the engineering of heart muscle". *Advanced Drug Delivery Review*. 2015.

Katia Bilodeau, and Diego Mantovani. "Bioreactors for Tissue Engineering: Focus on Mechanical Constraints. A Comparative Review". *Tissue Engineering*, Vol. 12, No. 8, 2006.

A. Marsano, C. Conficconi, M. Lemme, P. Occhetta, E. Gaudiello, E. Votta, G. Cerino, A. Redaelli, and M. Rasponi. "Beating heart on chip: a novel microfluidic platform to generate functional 3D cardiac microtissues". *Lab on a Chip*, 2016, 16. 599.

M. A. Mandel, "Surgical adhesives and sealants: Current technology and applications". *Plastic and Reconstructive Surgery*, 1997, Vol. 99, No. 6, 1780-1781.

T. A. E. Ahmed, E. V. Dare, and M. Hincke. "Fibrin: A Versatile Scaffold for Tissue Engineering Applications". *Tissue Engineering*, Part B, Vol. 14, No. 2, 2008.

Q. Ye, G. Zünd, P. Benedikt, S. Jockenhoewel, S. P. Hoerstrup, S. Sakyama, J. A. Hubbell, M. Turina. "Fibrin gel as a three-dimensional matrix in cardiovascular tissue engineering". *European Journal of Cardio-thoracic Surgery* 17, 2000, 587-591.

N. Tandon, C. Cannizzaro, E. Figallo, J. Voldman, and G. Vunjak-Novakovic. "Characterization of Electrical Stimulation Electrodes for Cardiac Tissue Engineering". *EMBS Annual International Conference* New York City, USA, Aug 30-Spt 3, 2006.

K. Jakab, C. Norotte, F. Marga, K. Murphy, G. Vunjak-Novakovic, and G. Forgacs. "Tissue engineering by self-assembly and bio-printing of living cells". *Biofabrication*, 2, 022001, 2010.

W. H. Zimmermann, C. Fink, D. Kralisch, U. Remmers, J. Weil, T. Eschenhagen. "Three-Dimensional Engineered Heart Tissue from Neonatal Rat Cardiac Myocytes". *Biothechnology and Bioengineering*, Vol. 68, No. 1, 2000.

G. Kensah, I. Gruh, J. Viering, H. Schumann, J. Dahlmann, H. Meyer, D. Skvorc, A. Bär, P. Akhyari, A. Heisterkamp, A. Haverich, and U. Martin. "A Novel Miniaturized Multimodal Bioreactor for Continuous In Situ Assessment of Bioartificial Cardiac Tissue During Stimulation and Maturation". *Tissue Engineering*, Part C, Vol. 17. No. 4, 2011.

H. Zhao, L. Ma, J. Zhou, Z. Mao, C. Gao, and J. Shen. "Fabrication and physical and biological properties of fibrin gel derived from human plasma". *Biomed. Mater.*, 3, 2008, 015001.

A. Hansen, A. Eder, M. Bönstrup, M. Flato, M. Mewe, S. Schaaf, B. Aksehirlioglu, A. Shwörer, J. Uebeler, T. Eschenhagen. "Development of a Drug Screening Platform Based on Engineered Heart Tissue". *Circulation Research*, 2010.

W. H. Zimmermann, K. Schneiderbanger, P. Schubert, M. Didié, F. Münzel, J. F. Heubach, S. Kostin, W. L. Neuhuber, T. Eschenhagen. "Tissue Engineering of a Differentiated Cardiac Muscle Construct". *Circulation Research*, 2002.

R. K. Birla, Y. C. Huang, R. G. Dennis. "Development of a Novel Bioreactor for the Mechanical Loading of Tissue-Engineered Heart Muscle". *Tissue Engineering*, Vol. 13. No. 9, 2007.

Stefan Jockenhovel and Thomas C. Flanagan. "Cardiovascular Tissue Engineering Based on Fibrin-Gel-Scaffolds". 2014.